

MMP2 and MMP9 Activity Is Crucial for Adult Visual Cortex Plasticity in Healthy and Stroke-Affected Mice

 Ipek Akol,¹ Evgenia Kalogeraki,^{1,2} Justyna Pielecka-Fortuna,¹ Merle Fricke,¹ and  Siegrid Löwel^{1,2,3}

¹Department of Systems Neuroscience, Johann-Friedrich-Blumenbach Institut für Zoologie und Anthropologie, Universität Göttingen, D-37075 Göttingen, Germany, ²Collaborative Research Center 889, Universität Göttingen, D-37075 Göttingen, Germany, and ³Göttingen Campus Institute for Dynamics of Biological Networks, Universität Göttingen, D-37073 Göttingen, Germany

A fundamental regulator of neuronal network development and plasticity is the extracellular matrix (ECM) of the brain. The ECM provides a scaffold stabilizing synaptic circuits, while the proteolytic cleavage of its components and cell surface proteins are thought to have permissive roles in the regulation of plasticity. The enzymatic proteolysis is thought to be crucial for homeostasis between stability and reorganizational plasticity and facilitated largely by a family of proteinases named matrix metalloproteinases (MMPs). Here, we investigated whether MMP2 and MMP9 play a role in mediating adult primary visual cortex (V1) plasticity as well as stroke-induced impairments of visual cortex plasticity in mice. In healthy adult mice, selective inhibition of MMP2/9 for 7 d suppressed ocular dominance plasticity. In contrast, brief inhibition of MMP2/9 after a cortical stroke rescued compromised plasticity. Our data indicate that the proteolytic activity of MMP2 and MMP9 is critical and required to be within a narrow range to allow adult visual plasticity.

Key words: extracellular matrix; MMP; ocular dominance plasticity; plasticity; stroke; visual cortex

Significance Statement

Learning and recovery from injuries depend on the plasticity of neuronal connections. The brain's extracellular matrix (ECM) provides a scaffold for stabilizing synaptic circuits, while its enzymatic proteolysis is hypothesized to regulate homeostasis between stability and reorganizational plasticity. ECM digestion is facilitated by a family of matrix metalloproteinases (MMPs). Here, we show that treatments that inhibit MMP2/9 can either inhibit or rescue cortical plasticity depending on cortical state: in the visual cortex of healthy adult mice, inhibition of MMP2/9 suppressed cortical plasticity. In contrast, brief inhibition of MMP2/9 after a stroke rescued compromised plasticity. Our data provide strong evidence that an optimal level of MMP2/9 proteolytic activity is crucial for adult visual plasticity.

Introduction

Ocular dominance (OD) plasticity induced by monocular deprivation (MD) has been one of the major paradigms for studying experience-dependent cortical plasticity since the first observations nearly six decades ago (Hubel and Wiesel, 1962). In the mammalian primary visual cortex (V1), neurons of the binocular zone respond to stimulation of both eyes. In rodents, the contralateral eye dominates visual cortical responses, which can be

modified by depriving the dominant eye of vision for a period of time (Dräger, 1978). Under standard cage (SC) conditions, OD plasticity decreases with age and is usually absent in mice older than postnatal day (P)110 (Lehmann and Löwel, 2008; Sato and Stryker, 2008). In SC mice, OD plasticity is most pronounced during the critical period (P21–P40) and mediated by a decrease in deprived eye V1 responses after 3–4 d of MD, called juvenile plasticity (Frenkel and Bear, 2004; Espinosa and Stryker, 2012; Levelt and Hübener, 2012). OD plasticity is still present in early adulthood (P70–P110) but mechanistically different: an increase of nondeprived eye V1 responses governs the shift in OD and requires at least 7 d of MD.

The tightly regulated plasticity of V1, as well as of other brain circuits, is of utmost importance for adaptation and survival of an organism in an ever-changing environment. An important challenge in neuroscience remains to identify the mechanisms regulating these dynamics in both health and disease. In the last two decades, it has become clear that many key mechanisms underlying plasticity are found in the interactions with the extracellular space surrounding neuronal cells. The extracellular

Received Mar. 25, 2021; revised Sep. 6, 2021; accepted Oct. 9, 2021.

Author contributions: J.P.-F. and S.L. designed research; I.A. and E.K. performed research; I.A. and M.F. analyzed data; I.A., E.K., J.P.-F., and S.L. edited the paper; I.A. and S.L. wrote the paper.

This work was supported by the German Research Foundation via the CRC 889 ("Cellular Mechanisms of Sensory Processing") (project B5; to S.L.) and by the Bundesministerium für Bildung und Forschung Grant 01GQ0810 (to S.L.). We thank Dr. Kalina Makowiecki for her guidance regarding statistical analyses, Natalie Gloveli for performing WFA stainings, Matthias Schink for excellent animal care and technical support, and the entire Löwel lab for inspiring discussions.

The authors declare no competing financial interests.

Correspondence should be addressed to Siegrid Löwel at sloewel@gwdg.de.

<https://doi.org/10.1523/JNEUROSCI.0902-21.2021>

Copyright © 2022 the authors

matrix (ECM) is a key regulator of both juvenile and adult plasticity. Restructuring of ECM by matrix metalloproteinases (MMPs), a family of zinc binding, multidomain endopeptidases, allows synaptic and circuit level reorganization (Berardi et al., 2004; Ethell and Ethell, 2007; Reinhard et al., 2015). In the CNS, MMPs also critically influence neuronal function through proteolytic processing of numerous ECM molecules, growth factors, cytokines, chemokines, and cell adhesion molecules (Ethell and Ethell, 2007; Huntley, 2012).

Previously, a rapid change in ECM protein composition was reported during OD plasticity in juvenile mice (Kelly et al., 2015), and MMPs were shown to be essential for open eye potentiation during 7 d of MD in juvenile rats (Spolidoro et al., 2012). In particular, our lab has reported that blocking the homeostatic activity of MMPs led to impairment of plasticity, highlighting the importance of accurate regulation of MMP activity for allowing adult visual cortex plasticity (Pielecka-Fortuna et al., 2015). Yet, excessive and prolonged activity of these enzymes is a major pathologic component of many CNS injuries and diseases such as stroke, neuroinflammation and demyelination (Rosenberg, 2002; Dityatev et al., 2010; Huntley, 2012; Reinhard et al., 2015). Increased MMP activity was reported within 24 h of a photothermally (PT)-induced stroke, and immediate treatment with a broad-spectrum MMP inhibitor rescued the stroke-induced impairment of both visual cortex (Greifzu et al., 2011; Pielecka-Fortuna et al., 2015) and barrel cortex plasticity (Cybulska-Klosowicz et al., 2011; Liguz-Leczna et al., 2012).

Although the critical role of MMPs for cortical plasticity and its impairment has become clearer in recent years, our understanding of the specific members of the MMP family that regulate visual cortex plasticity in health and disease is far from complete.

Of the 25 known MMPs, MMP2 and MMP9 are relatively abundant in the cortex and share the same substrates such as components of the ECM, adhesion molecules, cell surface receptors, growth factors, and other proteinases (Yong, 2005; Ethell and Ethell, 2007; Reinhard et al., 2015). MMP2 and MMP9 are secreted MMPs, and they restructure the ECM into a more permissive environment through proteolytic processing of numerous ECM molecules on synaptic activity (Ethell and Ethell, 2007). In the visual cortex, MMP9 expression has been detected with the peak expression pattern occurring at P0–P14, and MD increases MMP9 mRNA in cortex (Spolidoro et al., 2012). On the other hand, MMP2 is expressed in the CNS at higher basal levels than MMP9, and MMP2 is thought to function in OD plasticity without mRNA upregulation (Reinhard et al., 2015).

It was reported that MMP9 regulates experience-dependent plasticity and ECM remodeling in juvenile mice (Kelly et al., 2015), while light reintroduction after dark exposure was shown to increase the activity of MMP9 and reactivate plasticity in the adult visual cortex (Murase et al., 2017). In both humans and rodents, MMP2 and MMP9 are implicated in the pathology of brain injury by reports of elevated activity after ischemia (Rosenberg et al., 1998; Castellanos et al., 2003; Horstmann et al., 2003; Gu, 2005; Yang et al., 2010; Yang and Rosenberg, 2015).

We therefore investigated the role of MMP2/9 activity for visual cortex plasticity in adult (>P70) mice under various conditions using a combination of *in vivo* optical imaging of intrinsic signals and behavioral vision tests. We show that in the healthy brain, application of the MMP2/9-specific inhibitor SB3CT during MD prevented both OD plasticity and experience-enabled enhancements of the optomotor response of the nondeprived eye. In contrast, brief inhibition of MMP2/9 after a localized

lesion in primary somatosensory cortex (S1) completely rescued visual cortex plasticity. Together, these results provide *in vivo* evidence that an optimal level of MMP2/9 proteolytic activity is crucial for adult visual cortex plasticity in both health and disease.

Materials and Methods

Animals

All experimental procedures were approved by the local government: Niedersächsisches Landesamt für Verbraucherschutz und Lebensmittelsicherheit. Male and female wild-type C57BL6/J mice were obtained from the mouse colony of the central animal facility of the University Medical Center, Göttingen, Germany. All mice were housed with a 12/12 h light/dark cycle, with food and water available *ad libitum*.

Seven-day inhibition groups

Mice ($n = 19$, P70–P90) were housed in SCs (26 × 20 × 14 cm) in groups of three to four until the start of experiments. They were housed individually from day 0 (D0) of MD/noMD for 7 d of MD.

PT/sham groups

Mice ($n = 35$, P70–P90) were housed individually after PT or sham surgery and induction of MD/noMD on d0 for 7 d of MD.

Behavioral vision tests

In order to assess basic parameters of spatial vision, and their experience-induced changes in mice, both spatial frequency and contrast sensitivity thresholds of the optomotor reflex were measured using a commercially available virtual-reality optomotor setup (Prusky et al., 2004). Briefly, the experimental animals were randomly picked and placed on a round elevated platform in the middle of a box composed of four monitors and could freely move. Mirrors are positioned at both the bottom and the top of the box to create the perception of an endless cylinder for the mouse. A rotating virtual cylinder with moving vertical sine wave gratings (drift speed of 12°/s) was projected on the monitors. The animals reflexively track the moving gratings by head and upper body movements for as long as they can see the gratings. Spatial frequency at full contrast, and contrast at six different spatial frequencies [0.031, 0.064, 0.092, 0.103, 0.192, and 0.272 cycles/° (*cyc/°*)] was varied by the experimenter until the threshold of tracking was determined. Measured contrast sensitivity values were converted into Michelson contrasts as described previously (Prusky et al., 2004), and matched to the animal ID after measurements to enable blind data analyses. Behavioral testing was performed daily for 7 d in all mice, starting before MD (D0) in the MD groups to track any experience-enabled enhancement of visual capabilities. We always measured reflex thresholds through one eye [the nondeprived (left) eye of MD mice after MD, and the left eye of noMD mice] by exploiting the fact that the optomotor reflex is elicited only by temporal to nasal grating movements (Prusky et al., 2004).

MD

ODP was induced by depriving the contralateral (right) eye for 7 d as described previously (Cang et al., 2005; Pielecka-Fortuna et al., 2015). Mice were box-anesthetized with 2% isoflurane in a mixture of O₂/N₂O (75%/25%), their eyelids were sutured, and the animals were returned to their home cage for recovery. In stroke animals, MD was performed directly after the induction of a PT stroke (Greifzu et al., 2011; Pielecka-Fortuna et al., 2015). Mice were controlled daily to ensure the deprived eye remained closed. In case of an open MD eye, animals were removed from additional experiments.

Administration of the gelatinase (MMP2 and MMP9)-specific inhibitor SB3CT

To specifically inhibit the activity of MMPs 2 and 9 in the visual cortex, the specific inhibitor SB3CT [chemical name: 2-[[[(4-phenoxyphenyl)sulfonyl] methyl]-thiirane; formula: C₁₅H₁₄O₃S₂; SelleckChem] was

used and prepared as previously described with minor modifications as specified below (Brown et al., 2000; Gu et al., 2005).

Mice were injected intraperitoneally with either 25 mg/kg SB3CT (in 10% DMSO, 2% cyclodextrin in 0.9% saline) to a total volume of 200 μ l, or with 200 μ l vehicle (10% DMSO, 2% cyclodextrin in 0.9% saline) that was filtered [0.2- μ m sterile hydrophilic cellulose acetate (CA) membrane; Sartorius AG]. This type of systemic application of SB3CT was used before and shown to successfully inhibit both MMP2 and MMP9 activity in the brain tissue (Bonfil et al., 2006; Cui et al., 2012; Ranasinghe et al., 2012; Jia et al., 2014; Cai et al., 2017). The injections were administered daily for 7 d, starting 1 h after MD/no MD in the 7-d inhibition group. The mice receiving a PT/sham stroke induction were injected only once, 1 h after surgery. The inhibitor injections did not lead to any observable behavioral changes: during the routine monitoring and optomotor measurements, it was impossible for the experimenter to recognize the treatment that a particular experimental animal had received.

Induction of a PT stroke

The PT stroke was always induced in the left S1, i.e., in the same hemisphere where we recorded V1 activation, using the Rose Bengal technique (Watson et al., 1985) as described previously (Greifzu et al., 2011; Pielecka-Fortuna et al., 2015). This technique allows lesions with highly reproducible localization and size. Briefly, mice were box-anesthetized with 2% isoflurane in a mixture of 1:1 O₂/N₂O. During surgery, anesthesia was maintained at 0.8–1% isoflurane in 1:1 of O₂/N₂O delivered via an inhalation mask. The body temperature was maintained at 37°C using a heating pad and the mice were placed in a stereotaxic frame. The skin above the skull was incised, and an optic fiber bundle (aperture: 1.0 mm) mounted on a cold light source (Schott KL 1500) was positioned 2 mm lateral to the midline and 1 mm posterior to the bregma. A total of 100- μ l rose bengal dye (0.1%, in 0.9% saline) was injected intravenously into the tail vein. After a 5-min wait, the exposed area was illuminated (or not illuminated for sham-lesion experiments) for 15 min. Afterwards, the skin above the skull was sutured and animals were returned to their home cage for recovery. Lesion size was determined at the end of the behavioral and optical imaging experiments by glial fibrillary acidic protein (GFAP) immunostaining (Lai et al., 2014).

Optical imaging of intrinsic signals

Surgery

Mice were box-anesthetized with 2% halothane in a mixture of O₂/N₂O (1:1). The animals received injections of atropine (Franz Köhler, 0.3 mg/mouse, s.c.), dexamethasone (Ratiopharm, 0.2 mg/mouse, s.c.), and chlorprothixene (Sigma, 0.2 mg/mouse, i.m.) and were placed in a stereotaxic apparatus. The body temperature was maintained at 37°C and the heart rate was monitored throughout the experiment using the attached electrocardiography. Lidocaine (2% xylocaine gel, AstraZeneca GmbH) was applied to the scalp before incisions. The skin over the visual cortex was incised, and the exposed area was covered with low-melting point agarose (2.5% in 0.9% NaCl) and a glass coverslip to create a suitable optical surface and to prevent the skull from drying. After the surgery, anesthesia was reduced and kept at 0.4–0.6% halothane in 1:1 O₂/N₂O.

Optical imaging

Mouse visual cortical responses were recorded through the skull using the “Fourier”-imaging method developed by Kalatsky and Stryker (Kalatsky and Stryker, 2003) and optimized for the assessment of OD plasticity (Cang et al., 2005; Pielecka-Fortuna et al., 2015). In this method, a temporally periodic stimulus is continuously presented to the animal, and visual cortical responses at the specific stimulus frequency are extracted by Fourier analysis. Optical images of intrinsic cortical signals were obtained using a CCD-camera (coupled charged device; Dalsa 1M30) controlled by custom software. In order to visualize the surface vascular pattern, V1 was first illuminated by green light (550 \pm 10 nm) using a 135 \times 50-mm lens configuration (Nikon) for hemisphere recordings.

After acquisition of a surface image of blood vessels, the camera was focused 600 μ m below the pial surface, illumination was switched to the red wavelength (610 \pm 10 nm) and an additional red filter was

interposed between the camera and the objective to minimize light scatter. Frames were acquired at a rate of 30 Hz, temporally binned to 7.5 Hz, and stored as 512 \times 512-pixel images after spatial binning of the camera image.

Visual stimuli

We presented 2° wide drifting horizontal bars to the animal at a distance of 25 cm on a high refresh-rate monitor (Hitachi, ACCUVUE, HM-4921-D, 20 inches). The distance between the two bars was 70°, and they were presented at a temporal frequency of 0.125 Hz. To enable the calculation of OD, the visual stimulus was restricted to the binocular visual field of the left V1 (–5° to +15° azimuth, 0° azimuth corresponding to frontal direction), and either the left or the right eye was stimulated in alternation.

Data analysis

Fourier analysis was used to extract the signal at the stimulation frequency using custom software and visual cortical maps from the acquired frames were calculated (Kalatsky and Stryker, 2003). The phase component of the signal was used to calculate retinotopy, while the amplitude component, representing the intensity of neuronal activation (expressed as fractional change in reflectance $\times 10^{-4}$), was used to calculate OD.

First, the ipsilateral eye magnitude map was smoothed to reduce pixel shot noise with low-pass filtering using a uniform kernel of 5 \times 5 pixels. Then, a threshold was applied at 30% of peak response amplitude to eliminate background noise. Afterwards, an OD index (ODI) for every pixel in this region was calculated as: $(C - I)/(C + I)$, with C and I representing the response magnitude of each pixel to visual stimulation of the contralateral and ipsilateral eye, respectively (Cang et al., 2005). The ODI ranges from –1 to +1, with negative values representing ipsilateral, and positive values representing contralateral dominance. An ODI value was computed as the average of the OD scores of all responsive pixels (all pixels with response amplitude above 30% of peak response). Consequently, ODIs were calculated from blocks of four runs in which the averaged maps for each eye had at least a response magnitude of 1×10^{-4} . All ODI values of one animal (typically three to five) were averaged for further quantification and data display.

In the polar maps, hue encodes visual field position (retinotopy) and brightness encodes the magnitude of the visual responses. The quality of the retinotopic maps was assessed by the calculation described previously (Cang et al., 2005). The most responsive area within V1 was selected by thresholding at 30% of peak response amplitude of the activity map. For each of the pixels within this area the difference between its visual field position and the mean position of its surrounding 24 pixels was calculated. For maps of high quality, the position differences were quite small because of smooth progression. The standard deviation of the position difference was then used as an index of the quality of retinotopic maps with small values indicating high map quality and vice versa.

To ensure objective and unbiased data analyses, a second person (experimenter 2) who was blinded for the drug treatment, independently analyzed the imaging data. This was necessary because the drug solution needed to be prepared freshly and administered immediately. Therefore, it was not possible that another lab member prepared and coded the syringes, so that experimenter 1 (who performed the imaging experiments) needed to prepare the drugs and then, of course, was no longer blind toward the treatment. The imaging results obtained by experimenters 1 and 2 were quantitatively compared, and yielded essentially similar results, indicating that experimenter 1's knowledge of the injected drug/vehicle did not bias our optical imaging results. Tables comparing the two independent analyses are provided as the Extended Data Figures 2-1 and 5-1.

Perfusion and tissue preparation

Following optical imaging experiments, mice were deeply anesthetized with an intraperitoneal injection of 50 mg/kg pentobarbital and perfused transcardially with PBS (pH 7.4, 0.1 M) for 2 min followed by 4% paraformaldehyde (pH 7.4) for 8 min. The brain was removed and postfixed in 4% paraformaldehyde in PBS (pH 7.4) for 1 d, then transferred to a 10%

sucrose solution in PBS for 1 d followed by a 30% sucrose solution in PBS for 1 or 2 d (at 4°C). The brains were frozen in methylbutane at –40°C and stored at –80°C; 40- μ m-thick coronal brain sections were cut using a microtome.

Immunohistochemistry

GFAP staining of PT lesions

To analyze the size and the position of the PT-induced lesion, immunostaining with an antibody against GFAP (rabbit polyclonal antibody to GFAP; Immunologic Sciences) was performed as described previously (Lai et al., 2014; Kalogeraki et al., 2016). To determine size and location of the cortical lesions every third section was analyzed under a fluorescent microscope (Axioskop 50, Carl Zeiss) using AxioVision (AxioVs 40 4.5.0.0.). Animals in which the lesion extended into the white matter or V1 were excluded from further analyses.

Wisteria floribunda agglutinin (WFA) staining of perineuronal nets (PNNs). PNNs were labeled histochemically by WFA, an established marker for PNNs (Härtig et al., 1992) by *N*-acetylgalactosamine binding. Per mouse, three coronal brain sections that included V1 (\approx 2.70–3.88 mm posterior to bregma) were analyzed. The chosen brain sections were washed with 0.1 M PB three times for 10 min, before being incubated in a blocking solution (10% donkey serum, 0.3% Triton X-100 in PB, pH 7.4) for 30 min at room temperature. After blocking, the brain sections were incubated with biotin-conjugated lectin WFA (Sigma, dilution 1:1000) antibody in 0.1 M PB including 0.3% Triton X-100 at 4°C overnight. The next day, the sections were washed 3 times in 0.1 M PB at room temperature and incubated with the secondary antibody Cy3-conjugated streptavidin (Jackson ImmunoResearch, dilution 1:1000) in 0.1 M PB including 0.3% Triton X-100 light protected for 2 h at room temperature. Afterwards, the brain sections were washed again three times in 0.1 M PB and transferred on a microscope slide and dried for 30 min. The dried brain sections were mounted with Fluoromount (Southern Biotech), over which a glass cover slip was placed. In the mounting medium 4'0,6-diamidin-2-phenylindol (DAPI) was included for fluorescent staining of all cell nuclei.

Using a fluorescence microscope (Axio Imager.M2, Zeiss) pictures of the stained sections were taken for PNN quantification. The location of V1 was identified on the sections with the help of a mouse brain atlas (Paxinos and Franklin, 2001). The exposure time for the acquisition was set for every section to minimize differences in external conditions. The images of the sections were acquired using Neurolucida (version 10.51, MBF Bioscience) and a 10 \times objective. The filters were DAPI (Zeiss 49) excitation: 335–383 nm, emission: 420–470 nm and DSred (Cy3, Zeiss43) excitation: 533–558 nm, emission: 570–640 nm. A two-dimensional image of V1 was taken of three brain sections per animal. The quantification of the WFA-positive PNN cells was acquired using Fiji (Schindelin et al., 2012). A set frame was used to ensure equal conditions for counting PNNs in all sections. The area of V1 used for counting was measured with Fiji.

Statistical analyses

Representative figures of optical imaging were prepared on Adobe Illustrator CS6. GraphPad Prism 8.4.0 and IBM SPSS 24.0 were used for statistical analyses. Graphs were prepared using GraphPad Prism v8.4.0.

In the first part of the study, ODI, and maximum V1 activation from contralateral and ipsilateral eyes were analyzed using two-way ANOVA with between-subjects factors of injection and MD, and followed up with univariate ANOVAs for each dependent variable. Significant two-way interactions in the univariate ANOVAs were followed up with Sidak-corrected multiple comparisons to examine whether inhibitor injection had an effect on OD plasticity. The enhancement of spatial frequency thresholds of the optomotor reflex was analyzed with three-way mixed ANOVA with between-subjects factors of injection (vehicle, inhibitor) and MD (noMD, MD), and repeated measures of days (d0–d7). To examine the effects of inhibitor injection and MD on the improvement of spatial frequency threshold over days on MD, significant three-way interactions (injection \times MD \times day) were followed up by Sidak-corrected tests for simple effects of injection within each level of MD and day, and, of MD within each level of injection and day,

respectively. Contrast sensitivity thresholds were analyzed using four-way mixed ANOVA with between-subjects factors of injection and MD, repeated measures of day (d0 and d7), and the six spatial frequencies at which the contrast sensitivity was examined. To analyze how injection and MD affects the changes in contrast thresholds, significant interactions were followed up by Sidak-corrected tests for simple effects of injection within each level of MD, spatial frequency and day; and of MD within each level of injection, spatial frequency and day, respectively.

In the second part of the study, ODI and maximum V1 activation from contralateral and ipsilateral eyes were analyzed using multivariate ANOVA with between-subjects factors of PT, injection, and MD and followed up with univariate ANOVAs for each dependent variable. Significant two-way interactions in the univariate ANOVAs were followed up with Sidak-corrected tests for simple effects of injection within each level of MD, and of MD within each level of injection, to examine whether inhibitor injection had an effect on OD plasticity. The enhancement of spatial frequency thresholds was analyzed with three-way mixed ANOVA with between-subjects factors of injection (vehicle, inhibitor) and MD (noMD, MD), and repeated measures of days (d0–d7). To examine the effects of inhibitor injection and MD on the improvement of spatial frequency threshold over days on MD, significant three-way interactions (injection \times MD \times day) were followed up by Sidak-corrected multiple comparisons. Contrast sensitivity thresholds were analyzed using four-way mixed ANOVA with between-subjects factors of injection and MD, repeated measures of day (d0 and d7), and the six spatial frequencies at which the contrast sensitivity was examined. To analyze how injection and MD affects the changes in contrast thresholds, significant interactions were followed up by Sidak-corrected tests for simple effects of injection within each level of MD, spatial frequency and day; and of MD within each level of injection, spatial frequency and day, respectively.

Results

Treatment with the MMP2 and MMP9-specific inhibitor SB3CT prevented adult OD plasticity in mice.

Previously, our lab has demonstrated that MMPs play an important role in adult visual cortex plasticity by showing that broad spectrum inhibition of MMPs using GM6001 prevented OD plasticity after 7 d of MD in V1 of adult (three-month-old) mice (Pielecka-Fortuna et al., 2015).

To probe this mechanism further, here we investigated the role of MMP2 and MMP9 in adult visual cortex plasticity by using the specific inhibitor SB3CT. To test whether injections of SB3CT suppresses adult OD plasticity, we visualized V1 activation in adult mice (>P70) treated with either inhibitor or vehicle (control) during the 7 d of MD or noMD period by using *in vivo* intrinsic signal optical imaging (Fig. 1). To quantify experience-dependent V1-activation changes, we calculated an ODI for each mouse by comparing V1 activation in response to the stimulation of each eye. Figure 1 shows representative examples of optically recorded activity and polar maps after visual stimulation of the contralateral (right), and ipsilateral (left) eye, in the binocular region of the left V1 in both vehicle-treated control (vehicle; Fig. 1B,D), and SB3CT-treated adult mice (SB3CT; Fig. 1C,E). In all mice without MD (vehicle, $n = 4$; SB3CT, $n = 4$), the contralateral eye activated V1 more strongly, visible as a darker activity region, than the ipsilateral eye, regardless of the inhibitor treatment: average ODIs were positive, and warm colors prevailed the two-dimensional OD maps (Fig. 1B,C). Thus, inhibitor treatment did not influence basic V1 activation nor OD.

In contrast, after 7 d of MD (Fig. 1D,E), an OD shift was observed only in the control, but not the inhibitor (SB3CT-treated) group. In the control MD group (vehicle_MD, $n = 5$), both contralateral and ipsilateral eye stimulation elicited rather similar V1 activation, whereby visual responses to ipsilateral eye

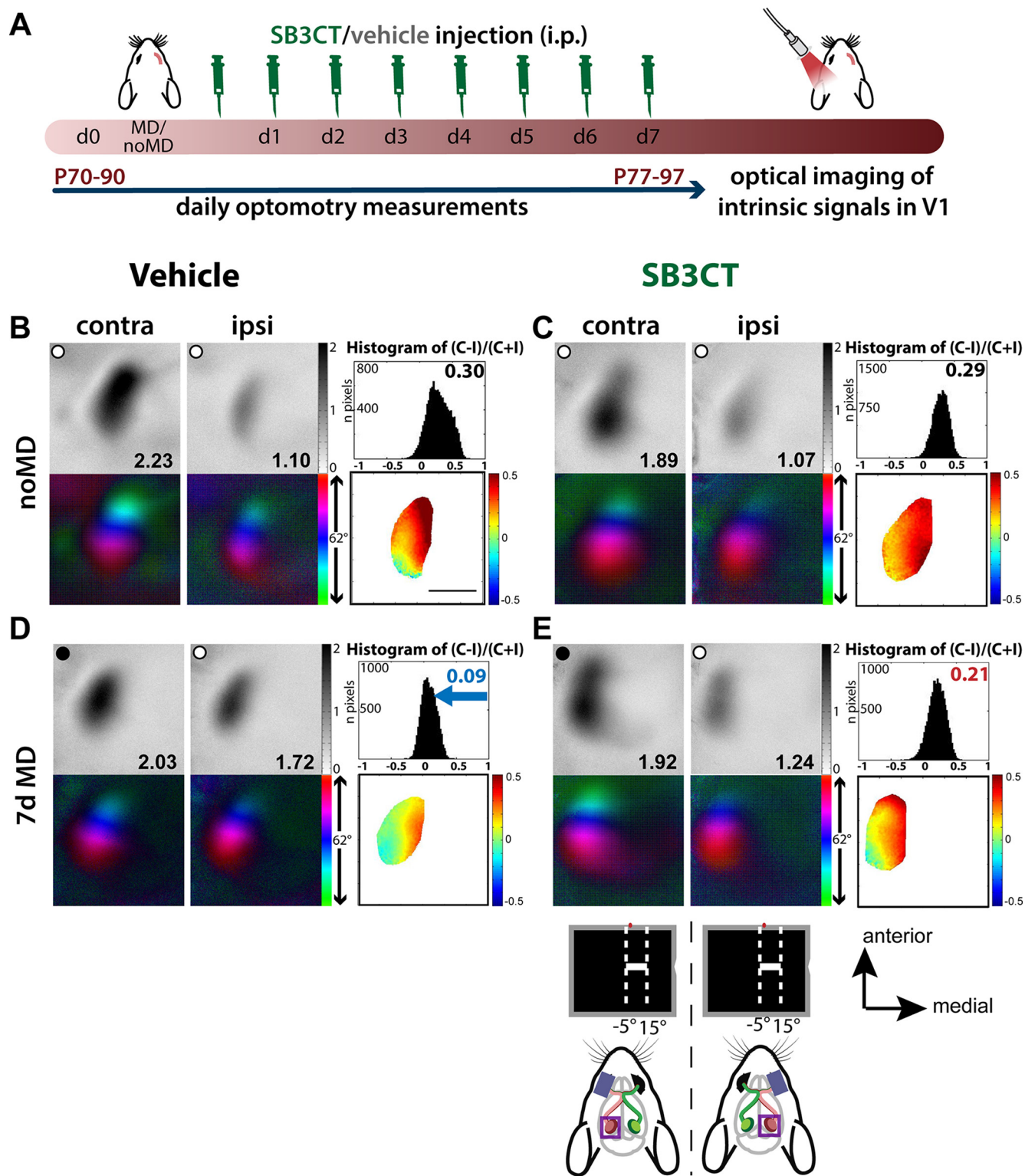


Figure 1. Treatment with the MMP2/9 inhibitor SB3CT during the MD period suppressed OD plasticity in adult mouse V1. **A**, Experimental timeline testing the effect of selective MMP2 and MMP9 inhibition on visual plasticity in healthy adult mice. Between P70 and P110, a group of mice received MD. From d0 (before MD), mice were checked daily for 7 d in the optomotor setup for the assessment of both spatial frequency and contrast sensitivity thresholds. One hour after MD, mice of all experimental groups were injected intraperitoneally with SB3CT or vehicle solution; injections continued until d7, when V1 activity was visualized using intrinsic signal optical imaging. **B–E**, Representative activity maps of the left binocular V1 and ODI values of vehicle-injected (**B, D**) or SB3CT-injected (**C, E**) mice. Greyscale-coded response magnitude maps, polar maps, two-dimensional OD maps, and histograms of OD scores including the average ODIs are illustrated. In mice without MD, activity patches evoked by stimulation of the contralateral eye were darker than those of the ipsilateral eye, the average ODI was positive, and warm colors prevailed in the OD maps, indicating contralateral dominance (**B, C**). In vehicle-injected mice, 7-d MD induced a strong OD shift toward the nondeprived (ipsilateral) eye (**D**): ipsilateral eye stimulation now caused darker V1-activity patches compared with noMD mice, colder colors appeared in the OD map, and average OD scores shifted to the left. In contrast, SB3CT-injected mice did not display OD plasticity (**E**). After MD, the contralateral eye continued to dominate V1 activation, warm colors continued to prevail in the OD map, and the average ODI was not changed (red) in SB3CT-treated mice (**E**). Scale bars: 1 mm.

stimulation were stronger compared with noMD mice. ODI histograms shifted to the left because ODI values were lower, and colder colors prevailed in the OD maps (Fig. 1D). In contrast, in SB3CT-treated MD mice (SB3CT_MD, $n = 6$), activity patches of the deprived, contralateral eye continued to dominate V1, and ODIs remained positive with warm colored two-dimensional OD maps (Fig. 1E), indicating suppressed OD plasticity on MMP2/9-specific inhibitor treatment.

Next, we performed a detailed quantification of the optical imaging data (Fig. 2). Analysis of ODIs showed significant main effects of MD, inhibitor, and their interaction (MD: $F_{(1,15)} = 28.2$, $p < 0.001$; inhibitor: $F_{(1,15)} = 7.0$, $p < 0.05$; interaction: $F_{(1,15)} = 6.1$, $p < 0.05$), indicating that the ODIs were dependent on the combination of injection and MD. Sidak-corrected multiple comparisons showed that in noMD mice, SB3CT injection had no significant effect on ODI nor maximum V1 activations, confirming that V1 activation and basic OD were not disrupted by the inhibitor (all $p > 0.05$; Fig. 2). As expected from literature values, vehicle-treated mice without MD had an average ODI of 0.3 ± 0.03 , whereas after 7 d of MD, their ODI decreased to 0.1 ± 0.01 ($p < 0.001$; Fig. 2A). In contrast, ODIs of MD and noMD SB3CT-treated groups were not different (0.3 ± 0.01 and 0.2 ± 0.04 , respectively; $p = 0.303$; Fig. 2A), indicating that MMP2/9 inhibitor injection prevented OD plasticity in adult mouse V1 (Fig. 2A).

To understand the mechanism underlying the experience-dependent network changes we analyzed the V1 responses in detail. In vehicle-treated mice, V1 activation after ipsilateral eye stimulation increased from $1.0 \pm 0.1 \times 10^{-4}$ $\Delta F/F$ without MD to $1.5 \pm 0.2 \times 10^{-4}$ $\Delta F/F$ after MD ($p < 0.01$; Fig. 2B). Thus, the OD shift was mediated by increased V1 responses on visual stimulation of the nondeprived eye, in line with previous literature on the typical V1-activation changes after 7 d of MD in young adult mice (Sawtell et al., 2003; Hofer et al., 2006; Sato and Stryker, 2008; Levelt and Hübener, 2012). In contrast, SB3CT-injected mice did not show a significant increase of nondeprived eye V1 responses after MD ($p > 0.05$), and the contralateral eye continued to dominate V1 responses ($p < 0.05$; Figs. 1E, 2B). Surprisingly, while V1 activation via the contralateral eye was similar to vehicle-treated mice in baseline (without MD), after MD, contralateral V1 activation of SB3CT-injected mice decreased compared with the noMD group ($p < 0.05$).

Moreover, we also tested the effect of MMP2/9 inhibition on ECM degradation, using WFA staining of perineuronal nets (PNNs) in V1 of vehicle, and SB3CT-treated adult mice. PNNs are an important component in the ECM and their degradation has been shown previously to enhance OD plasticity (Pizzorusso et al., 2002). To determine whether PNNs were altered on MMP2/9 inhibitor treatment, we counted WFA-positive PNNs on WFA-stained V1 sections (Fig. 3A). V1 of SB3CT-injected mice had significantly higher numbers of PNNs (SB3CT: 80.28 ± 15.86 PNN/mm², SB3CT_MD: 86.32 ± 8.23 PNN/mm²) compared with vehicle-injected mice (vehicle: 59.07 ± 7.89 PNN/mm², vehicle_MD: 64.72 ± 7.23 PNN/mm², $p = 0.037$, unpaired t test; Fig. 3B). Thus, we confirmed that our paradigm of systemic administration of the MMP2/9 inhibitor SB3CT indeed led to higher number of PNNs compared with control conditions.

To summarize, daily injections of SB3CT, a MMP2/9-specific inhibitor for the duration of a 7-d MD was sufficient to prevent OD plasticity in V1 of adult mice, most likely by suppressing the improvement of nondeprived eye responses in binocular V1. Overall, our data suggest that MMP2/9 proteolytic activity is critical for accommodating adult OD plasticity, possibly through ECM degradation.

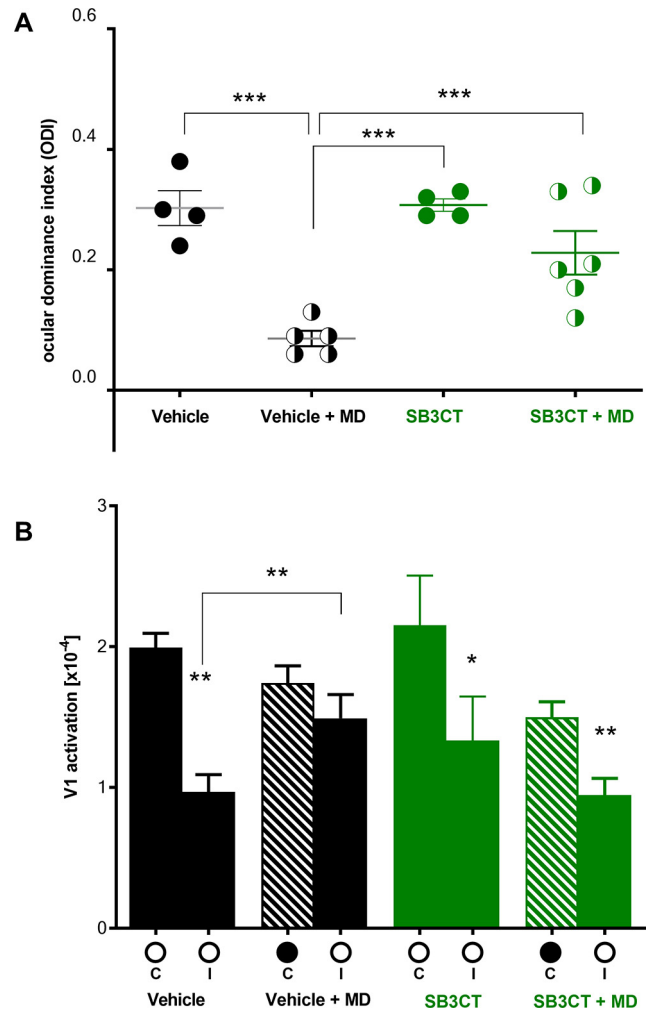


Figure 2. Quantification of ODIs (A) and V1 activation (B) in vehicle-injected (black) and SB3CT-injected (green) mice with or without MD. **A**, Administration of SB3CT for 7 d abolished OD plasticity in MD mice. Symbols represent ODI values of individuals; filled circles represent mice without MD and half-filled circles mice with MD; mean values are shown as horizontal lines. **B**, V1 activation (fractional change in reflectance $\times 10^{-4}$) elicited by stimulation of the contralateral (C) or ipsilateral (I) eye without and after MD (deprived eye is marked by a black filled circle on the x-axis). In vehicle-treated mice, the OD shift was primarily mediated by an increase of open (ipsi) eye responses in V1, while after SB3CT treatments, there was no significant increase in open eye responses of MD mice receiving injections. Multivariate ANOVA, followed up by Sidak-corrected multiple comparisons. Mean \pm SEM, * $p < 0.05$, ** $p < 0.01$, *** $p < 0.001$. Tables comparing the two independent analyses are provided as the Extended Data Figure 2-1.

Treatment with the MMP2 and MMP9-specific inhibitor SB3CT prevented experience-enabled improvements of basic visual abilities

To further understand the role of MMP2/9 proteolytic activity in the behavioral context of visual abilities, we have utilized the virtual reality optomotor setup. Spatial vision of rodents, i.e., basic parameters of visual capabilities, like the spatial frequency and contrast sensitivity thresholds of the optomotor reflex and their experience-enabled enhancements can be quantified by using optometry (Prusky et al., 2004, 2006).

To this end, all experimental mice were tested on d0 (before MD) to obtain a baseline value for spatial vision. Then, during the following 7 d of MD (or no MD), both spatial frequency and contrast sensitivity thresholds of the optomotor reflex were measured daily during monocular vision, in both vehicle-treated and SB3CT-treated animals.

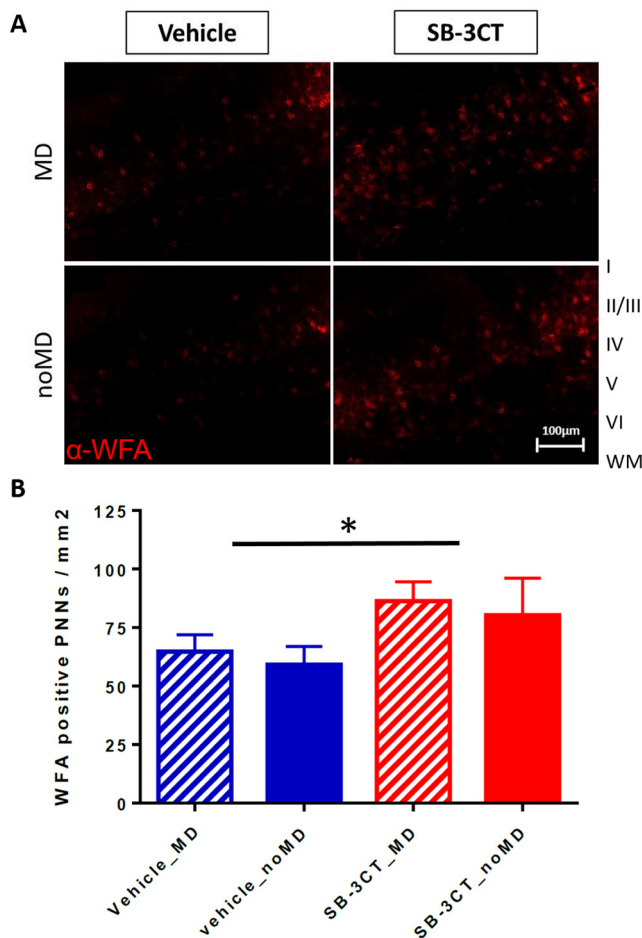


Figure 3. Daily injection of the MMP2/9-specific inhibitor SB3CT increased PNNs in V1, stained with WFA. **A**, WFA-positive staining of PNNs in vehicle-injected (left) and SB3CT-injected (right) mice. PNNs were identified by their shape and bright circular outline throughout the layers of V1. One example of each condition is displayed. On the right, noMD/MD conditions of vehicle-injected mice are shown. On the left, noMD/MD conditions of SB3CT-injected mice are shown. Scale bar: 100 μ m. **B**, Quantification of PNNs in V1. Number of WFA-positive PNNs were significantly higher in SB3CT-injected mice, regardless of MD. From each brain, three sections containing V1 were analyzed. ANOVA followed up by Sidak-corrected test for simple effects. Scale bar: 100 μ m. Mean \pm SEM, * p < 0.05, ** p < 0.01, *** p < 0.001.

The analysis of spatial frequency thresholds showed that there were significant main effects of MD, inhibitor, and time (MD: $F_{(1,15)} = 52.6$; inhibitor: $F_{(1,15)} = 21.3$; time: $F_{(1,41,21,12)} = 59.8$, all p < 0.001), which were qualified by significant three-way interactions (time \times injection \times MD: $F_{(7,105)} = 23.7$, p < 0.0001), indicating that the change in thresholds over 7 d depended on the combination of both injection and MD. There were also significant main effects of MD, inhibitor, time, and spatial frequency on contrast sensitivity thresholds (MD: $F_{(1,15)} = 28.9$; inhibitor: $F_{(1,15)} = 23.8$; time: $F_{(1,15)} = 73.9$; spatial frequency: $F_{(1,9,27,9)} = 219.8$; all p < 0.001), which were qualified by significant four-way interactions (time \times injection \times MD \times spatial frequency: $F_{(1,15)} = 13.2$). Thus, at each spatial frequency, contrast sensitivity thresholds between days 0 and 7 depended on the combination of both inhibitor treatment and MD. Baseline values on d0 were alike between all groups (all p > 0.05), and consistent with previous literature, but the effect of the drug over time varied depending on whether mice received MD or not (Prusky et al., 2004; Lehmann and Löwel, 2008).

As expected from previous publications (Prusky et al., 2006; Lehmann and Löwel, 2008; Pielecka-Fortuna et al., 2015), both

spatial frequency and contrast sensitivity thresholds did not change in noMD groups, and the MMP2/9 inhibitor treatment (SB3CT) did not affect basal visual capabilities of noMD mice over 7 d (for both spatial and contrast thresholds: p > 0.05). Thus, the SB3CT injections did not interfere with basal visual capabilities (Fig. 4).

Next, we focused on the effect of SB3CT on the experience-enabled improvements of visual abilities. Comparison of noMD and MD mice within the SB3CT-treated group showed that spatial frequency and contrast sensitivity thresholds at any spatial frequency did not improve significantly over 7 d (all p > 0.05). After 7 d of MD, the spatial frequency thresholds of SB3CT-treated MD mice increased by only $3.9 \pm 0.4\%$ (d0/d7: $0.38 \pm 0.002/0.39 \pm 0.003$ cyc/°; Fig. 4A). Consequently, SB3CT_MD mice had significantly lower values than vehicle-treated MD mice on d7 after MD (p < 0.05). In contrast, mean spatial frequency threshold of vehicle-injected MD mice increased by $16.8 \pm 0.02\%$ over 7 d of MD (d0/d7: $0.38 \pm 0.003/0.44 \pm 0.005$ cyc/°; contrast sensitivity, Table 1; Fig. 4). The significant improvement of MD on contrast sensitivity thresholds in vehicle-injected mice was observed at all six measured spatial frequencies (all p < 0.001).

In summary, treatment with the MMP2/9 inhibitor SB3CT for the duration of MD suppressed the experience-induced improvements of both the spatial frequency and the contrast sensitivity thresholds of the optomotor reflex of the open eye without modifying basic visual abilities. Our behavioral vision assessments thus highlight MMP2/9 as essential players in cortex-dependent experience-driven enhancements of visual capabilities.

A single injection of the MMP2 and MMP9-specific inhibitor SB3CT rescued stroke-induced visual plasticity impairments

We had previously described that a small PT lesion in the S1 can severely impair visual plasticity in V1 (Greifzu et al., 2011, 2014). Increased expression of MMP9 have been detected within hours to days following stroke in nonhuman primates (Heo et al., 1999), rats (Romanic et al., 1998; Rosenberg et al., 1998), and mice (Fujimura et al., 1999; Asahi et al., 2001; Turner and Sharp, 2016). Moreover, in acute stroke, MMP2 is activated as one of the first responses (Yang and Rosenberg, 2015). However, which MMPs are upregulated is highly dependent on the type, localization, and strength of the ischemic insult (Turner and Sharp, 2016). After a cortical stroke, cortical plasticity is compromised in the infarct and peri-infarct regions, but can be restored by broad-spectrum inhibition of MMPs in both somatosensory and visual cortex (Cybulska-Klosowicz et al., 2011; Liguz-Lecznar et al., 2012; Pielecka-Fortuna et al., 2015). We therefore examined whether also a brief treatment with the MMP2/9-specific inhibitor SB3CT can rescue visual cortex plasticity in adult mice after a PT stroke in S1.

To assess the size and location of the PT lesions, we conducted GFAP-immunofluorescence analyses. PT lesions were localized in the left S1, $\sim 1.1 \pm 0.2$ mm anterior from the anterior border of V1, 2.2 ± 0.2 mm lateral to the midline, and 1.1 ± 0.2 mm posterior to bregma. The average size of the lesions was 0.7 ± 0.1 mm in the mediolateral and 0.6 ± 0.1 mm in anterior-posterior directions. Our measurements revealed that there were no differences in lesion sizes nor locations between SB3CT-treated and vehicle-treated PT mice (t test, all p > 0.05).

As expected from our previous data, 7 d of MD did not induce OD shifts in the vehicle-injected PT-lesioned mice (PT_vehicle_MD, $n = 4$). The deprived, contralateral eye continued to yield darker activity patches in V1 compared with the

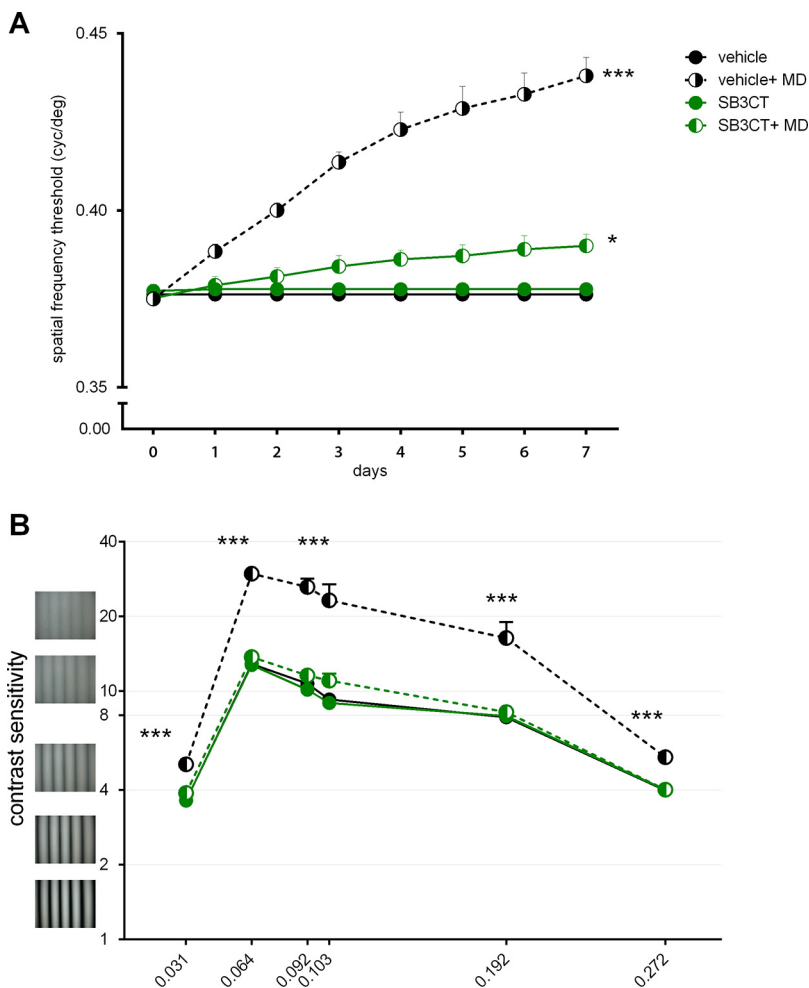


Figure 4. Injection of the MMP2/9 inhibitor SB3CT prevented experience-induced enhancements of both the spatial frequency (A) and contrast sensitivity (B) thresholds of the optomotor reflex of the open eye in adult mice after MD (half-filled circles). **A**, Spatial frequency threshold values in cyc/deg are plotted against days, for mice without (filled circles) and with MD (half-filled circles) for both vehicle-treated (black) and SB3CT-treated (green) mice. After 7 d of MD, spatial frequency thresholds improved significantly in vehicle-injected MD mice when compared with mice without MD and SB3CT-injected MD mice. In contrast, SB3CT-injected MD mice did not significantly increase thresholds until D7, while control MD mice improved significantly each day. Mice without MD did not show any change over days. Three-way mixed ANOVA was used, followed up by Sidak-corrected tests for simple effects. **B**, In vehicle-treated MD mice, contrast sensitivity thresholds of the open eye increased significantly after 7-d MD compared with both noMD mice (filled circles) and SB3CT-injected noMD mice (blue). SB3CT MD mice (blue, half-filled circles) had significantly lower contrast sensitivity thresholds than vehicle-injected mice (black, half-filled circles), similar to noMD mice (filled circles). Gratings left of the y-axis illustrate the contrast steps for a given (constant) spatial frequency. Four-way mixed ANOVA, followed up by Sidak-corrected tests for simple effects. Mean \pm SEM, * $p < 0.05$, ** $p < 0.01$, *** $p < 0.001$.

ipsilateral (open) eye, average ODIs remained positive and two-dimensional OD maps were still dominated by warm colors; all indicative of a typical contralateral eye dominance in binocular V1 (Fig. 5D). However, a single intraperitoneal injection of the MMP2/9 inhibitor SB3CT (PT_SB3CT_MD, $n = 5$) was able to rescue OD plasticity in PT-lesioned mice: V1 activation via the contralateral and ipsilateral eye were similar, ODI values decreased strongly, OD maps exhibited colder colors, and the ODI histograms shifted to the left (Fig. 5D).

We next quantified all optically recorded V1 maps (Fig. 6). There were significant main effects of MD and PT (MD: $F_{(1,27)} = 24.5$, $p < 0.001$; PT: $F_{(1,27)} = 5.2$, $p < 0.05$), and two-way interactions of MD, PT, and inhibitor injections on ODIs (MD \times PT: $F_{(1,27)} = 4.8$, $p < 0.05$; PT \times injection: $F_{(1,27)} = 5.4$, $p < 0.05$). Thus, the effect of MD and inhibitor depends on whether or not

the mice received a PT lesion, and inhibitor treatment alone did not have an effect on OD plasticity.

After MD, vehicle-treated PT mice had a mean ODI of 0.2 ± 0.03 ($n = 4$), similar to values recorded from noMD mice ($p > 0.05$). In contrast, the SB3CT-injected PT mice had a significantly lower mean ODI of 0.1 ± 0.02 ($n = 5$) after 7 d of MD ($p < 0.05$), indicating that OD plasticity, impaired by a localized S1 lesion, was rescued by a single injection of SB3CT in adult mice (Fig. 6A). Mice without MD of both PT and sham groups had similar ODI values (all $p > 0.05$).

In sham-lesioned mice, both MD groups had significantly lower ODI values than their noMD counterparts did (sham_vehicle: 0.2 ± 0.02 , sham_vehicle_MD: 0.1 ± 0.03 , $p < 0.01$; sham_SB3CT: 0.3 ± 0.04 , sham_SB3CT_MD: 0.1 ± 0.02 , $p < 0.01$). Importantly, a single dose of inhibitor did not prevent the OD shift induced by MD ($p > 0.05$; Fig. 6A), in contrast to our observations in nonlesioned mice after seven consecutive injections of SB3CT (Fig. 2).

To further examine the mechanisms rescuing OD plasticity after stroke, we analyzed V1 responses elicited by contralateral and ipsilateral eye stimulation. In SB3CT-treated PT mice, V1 activation via the contralateral eye decreased from $1.3 \pm 0.1 \times 10^{-4}$ $\Delta F/F$ (noMD) to $1.1 \pm 0.04 \times 10^{-4}$ $\Delta F/F$ after MD, while V1 activity via the ipsilateral eye increased from 0.7 ± 0.1 without MD to $0.9 \pm 0.1 \times 10^{-4}$ $\Delta F/F$ after MD. In the PT_vehicle_MD group, deprived eyes continued to dominate V1 activation (contralateral: noMD: $1.3 \pm 0.2 \times 10^{-4}$ $\Delta F/F$, MD: $1.1 \pm 0.2 \times 10^{-4}$ $\Delta F/F$; ipsilateral: noMD: $0.5 \pm 0.1 \times 10^{-4}$ $\Delta F/F$, MD: $0.8 \pm 0.2 \times 10^{-4}$ $\Delta F/F$; $p > 0.05$; Fig. 6B). V1 responses elicited by contralateral eye stimulation were significantly higher than those after ipsilateral eye stimulation in vehicle-treated PT mice with or without MD (PT_vehicle_MD/noMD, $p < 0.05$), in SB3CT-treated PT mice with MD. However, contralateral eye responses in V1 were reduced such that there was no significant difference in V1 activation between contralateral and ipsilateral eye stimulation (PT_SB3CT_MD contra: $1.07 \pm 0.04 \times 10^{-4}$ $\Delta F/F$, ipsi: $0.89 \pm 0.07 \times 10^{-4}$ $\Delta F/F$, $p > 0.05$; Fig. 6B). Thus, SB3CT treatment rescued OD plasticity in PT-lesioned mice, as there was a clear OD shift mediated by decreased V1 responses to deprived eye stimulation.

In summary, our data demonstrate that a single injection of the specific MMP2/9 inhibitor SB3CT, applied immediately after lesion induction, can rescue OD plasticity which is otherwise lost after a PT lesion in S1 (Greifzu et al., 2011). Taken together, our data confirm that an S1 stroke has long-range effects and compromises cortical plasticity in binocular V1 but also demonstrate for the first time that plasticity can be rescued by an immediate treatment with the MMP2/9-specific inhibitor SB3CT against upregulated MMP2/9 activity.

Table 1. Optometry-measured contrast sensitivity comparisons before and after MD

Spatial frequency (cyc/°)	Contrast sensitivity d0		[100/(%value*0.985)]	
	Vehicle	Vehicle_MD	SB3CT	SB3CT_MD
0.031	2.6 ± 0.05	3.7 ± 0.06	3.6 ± 0.03	3.7 ± 0.07
0.064	12.8 ± 0.15	11.8 ± 0.10	12.8 ± 0.25	11.7 ± 0.35
0.092	10.7 ± 0.10	10.3 ± 0.55	10.1 ± 0.38	9.9 ± 0.36
0.103	9.3 ± 0.39	9.0 ± 0.70	9.0 ± 0.21	9.2 ± 0.46
0.192	7.8 ± 0.39	7.1 ± 0.33	7.9 ± 0.07	7.2 ± 0.26
0.272	4.0 ± 0.04	3.8 ± 0.07	4.0 ± 0.03	3.7 ± 0.09
	d7			
0.031	3.6 ± 0.05	5.1 ± 0.25	3.6 ± 0.04	3.9 ± 0.08
0.064	12.9 ± 0.15	29.7 ± 1.25	12.7 ± 0.20	13.7 ± 0.71
0.092	10.7 ± 0.10	26.3 ± 2.09	10.1 ± 0.35	11.6 ± 0.61
0.103	9.26 ± 0.25	23.2 ± 3.76	9.0 ± 0.20	11.0 ± 0.76
0.192	7.9 ± 0.40	16.4 ± 2.64	7.9 ± 0.06	8.2 ± 0.36
0.272	4.0 ± 0.04	5.4 ± 0.18	4.0 ± 0.04	4.0 ± 0.10

A single injection of the MMP2/9-specific inhibitor SB3CT after a cortical lesion recovered experience-driven visual abilities.

As previously shown, a PT stroke in S1 prevented the experience-induced improvements of optomotor reflex thresholds of the nondeprived eye after MD (Greifzu et al., 2011), but enhancements of both spatial frequency and contrast thresholds could be rescued by a brief broad-spectrum inhibition of MMPs (Pielecka-Fortuna et al., 2015). To test whether a selective (and brief) inhibitor of MMP2/9 activity can also act therapeutically, we first acquired baseline optomotor thresholds, then induced the S1-stroke lesion, treated experimental animals with the MMP2/9 inhibitor SB3CT and continued with daily optomotor testing during the 7-d MD (or noMD) period in both PT-lesioned and sham-lesioned mice (Table 2; Fig. 7).

We observed significant main effects of MD, PT, and time ($p < 0.001$) on spatial frequency thresholds, which were qualified by significant four-way interactions of MD, surgery, inhibitor, and time, suggesting that the improvements in spatial frequency threshold over 7 d depended on the combination of PT, inhibitor, and MD ($F_{(1,26)} = 7.3$, $p = 0.01$; Greenhouse–Geisser corrected). There were also significant main effects of MD, time, and spatial frequency (p values < 0.001) on contrast sensitivity thresholds. These main effects were qualified by significant five-way interactions of MD, PT, inhibitor, spatial frequency, and time, indicating that the improvement of contrast sensitivity thresholds at each spatial frequency over 7 d depended on the combination of PT, inhibitor, and MD ($F_{(1.4,36.5)} = 10.6$, $p < 0.001$; Greenhouse–Geisser corrected). Our baseline values (before MD/stroke/treatment) were alike in all groups (all $p > 0.05$), and consistent with previous literature (Prusky et al., 2004; Lehmann and Löwel, 2008; Pielecka-Fortuna et al., 2015), and the effect of inhibitor varied depending on whether mice were subjected to PT and/or MD.

Follow-up tests indicated that the spatial frequency and contrast sensitivity thresholds of the optomotor reflex of PT-lesioned vehicle-treated (control) mice (PT_vehicle_MD, $n = 4$) remained unchanged over 7 d of MD (spatial frequency threshold: change: $0.5 \pm 0.1\%$, D0/7: $0.378 \pm 0.003/0.381 \pm 0.002$ cyc/°; contrast threshold, Table 3; both $p > 0.05$; Fig. 7). In contrast, SB3CT treatment rescued the experience-enabled optomotor enhancements after MD in PT mice (PT_SB3CT_MD, $n = 5$), both for spatial frequency thresholds (change: $14.3 \pm 1.7\%$; D0/7: $0.37 \pm 0.001/0.43 \pm 0.009$ cyc/°) and for contrast thresholds (Table 2; both $p < 0.001$; Fig. 7). The MD-induced threshold

improvements of PT_SB3CT_MD mice were also higher than without MD (both $p < 0.001$; Fig. 7). Together, these data indicate that a brief treatment with the MMP2/9 inhibitor SB3CT against excessive MMP2/9 activity within 24 h of a PT lesion in S1 rescued the otherwise impaired experience-induced enhancements of visual abilities in adult mice.

To exclude an effect of the surgical interventions on our results, we also analyzed the visual abilities of sham-treated mice (similar surgery but no PT lesion), and established that MD, as expected from previous literature, induced an experience-dependent increase in both spatial frequency and contrast sensitivity thresholds of the optomotor reflex, regardless of the injection (vehicle/SB3CT). Thus, a single SB3CT injection after MD did not interfere with experience-induced improvements of visual capabilities in sham control mice (all $p < 0.001$; Fig. 7), in contrast to seven injections of this selective MMP2/9 inhibitor (Fig. 2).

In summary, our behavioral vision assessments establish that upregulation of MMP2/9 after a localized cortical lesion in S1 contributes to the impairment of experience-driven improvements of optomotor thresholds in adult mice. Furthermore, MMP2/9 inhibition can potentially be used therapeutically to rescue compromised plasticity: a single injection of the selective MMP2/9 inhibitor SB3CT, administered 1 h after lesion induction, is sufficient to rescue the experience-enabled optomotor improvements.

Discussion

The objective of our study was to examine the role of MMP2 and MMP9 in adult visual cortex plasticity in both health and disease. We hypothesized that the proteolytic activity of MMP2 and MMP9 allows experience-induced neuronal plasticity in the healthy visual cortex, while the upregulation of these ECM-digesting enzymes upon a cortical lesion contributes to the observed impairments of visual cortical plasticity (Pielecka-Fortuna et al., 2015). To this end, we have used injections of the MMP2/9-specific inhibitor SB3CT and a combination of behavioral vision tests, *in vivo* optical imaging and immunohistochemistry. SB3CT was previously shown to be a highly selective and specific inhibitor of gelatinases MMP2 and MMP9, with the ability to cross the brain-blood barrier (Brown et al., 2000; Gu, 2005). Therefore, we would like to interpret our results of SB3CT treatment as showing that inhibition of MMP2 and MMP9 has a major effect on adult cortical plasticity in both health and disease. In particular, our results provide evidence that the activity of MMP2 and MMP9 is critical for visual plasticity in healthy adult animals, while their upregulation following a cortical lesion must be counteracted to accommodate visual plasticity in injured brains.

MMP2/9 in healthy visual cortex

In the healthy adult brain, remodeling of the ECM is an important regulator of synaptic function and plasticity (Frischknecht and Gundelfinger, 2012). An enhancement of OD plasticity following the degradation of the mature ECM was first documented in rat V1 (Pizzorusso et al., 2002, 2006). It has been established that maturation of the ECM contributes to the stability of existing nerve cell connections, while tightly regulated endogenous degradation can locally shift the balance toward plasticity, enabling new experience-induced changes (Gundelfinger et al., 2010; Reinhard et al., 2015). This enzymatic degradation is facilitated largely by MMPs, whereby the expression and activity of

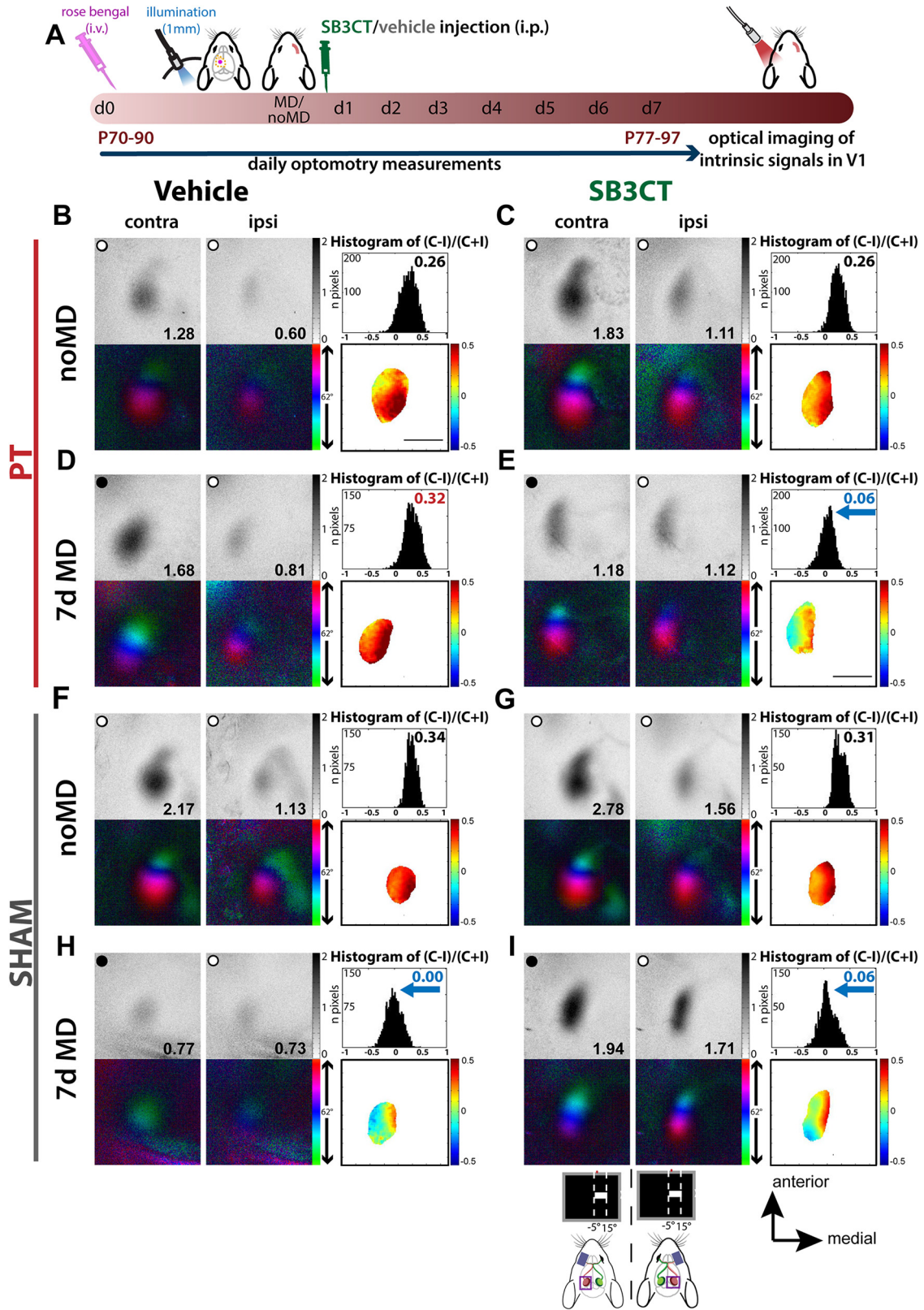


Figure 5. Brief treatment with the MMP2 and MMP9-specific inhibitor SB3CT rescued adult OD plasticity in V1 after a stroke in S1. **A**, The experimental design to test the effect of MMP2 and MMP9 inhibition on OD plasticity after a PT stroke in S1. A small (1 mm in diameter) lesion in S1 was induced on young adult mice (P70–P90) using PT. Shortly after (1 h), half of the PT mice received MD. One hour after MD, mice were injected with SB3CT or vehicle solution and returned to their home cages. Starting from d0 before MD, mice were checked daily in the optomotor setup for the assessment of spatial frequency and contrast sensitivity thresholds of the optomotor reflex for the following 7 d. On d7, optical imaging of intrinsic signals was performed, after which the mice were perfused, and the brains were harvested. After tissue preparation and immunohistochemistry, PT lesions were measured. Representative activity maps of binocular V1 and ODI values of the left hemisphere measured by optical imaging of intrinsic signals in PT-lesioned, one-time vehicle-injected (**B**, **D**) or SB3CT-injected (**C**, **E**), or sham-treated vehicle-injected (**F**, **H**) or SB3CT-injected (**G**, **I**), mice are displayed. In PT mice without MD (**B**, **C**), activity patches evoked by stimulation of the contralateral eye were darker than those of the ipsilateral eye, the average ODI was positive, and warm colors prevailed in the OD maps, indicating contralateral dominance in the left hemisphere binocular V1. Vehicle-injected PT mice with MD (deprived eye is marked by black filled

various MMPs changes depending on the brain region and developmental stage (Ethell and Ethell, 2007; Reinhard et al., 2015). MMP9 has been extensively characterized in the mouse brain, and it is implicated in mediating plasticity in various brain regions, including juvenile and adult visual cortex (Yong, 2005; Huntley, 2012; Kelly et al., 2015; Reinhard et al., 2015; Murase et al., 2017). MMP2 also has a similar structure and substrate specificity as MMP9, and both MMP2 and MMP9 expression tend to co-localize at individual excitatory synapses (Huntley, 2012). In response to long-term potentiation (LTP) induction, MMP9 rapidly becomes proteolytically active at perisynaptic sites and is essential for maintenance of LTP and local remodeling (Meighan et al., 2006; Nagy et al., 2006).

With respect to visual cortical plasticity after MD, MMP9 was previously shown to be required for the increase of open eye responses in juvenile mice (Kelly et al., 2015). Here, we report that OD plasticity in adult V1 is also depending on MMP2/9 activity, because treatment with the MMP2 and MMP9-specific inhibitor SB3CT blocked plasticity and prevented an increase of V1 activation through the open, nondeprived eye. This observation expands previous findings from our lab, in which chronic treatment with a broad-spectrum MMP inhibitor prevented open eye potentiation and compromised OD plasticity (Pielecka-Fortuna et al., 2015). Thus, specific inhibition of MMP2/9 led to a similar level of suppression in open eye potentiation in V1 of adult mice following MD.

It is plausible that the effects observed with the broad-spectrum inhibition of MMPs were, in fact, predominantly because of the inhibition of MMP2/9, given that the results obtained in the two studies are very similar. Since MMP2 has low basal levels of activity in mouse cortex (Wilczynski et al., 2008), including the visual cortex (Murase et al., 2017), MMP9 might play a bigger role for OD plasticity in the adult visual cortex.

Juvenile *Mmp9* knock-out mice manifest reduced excitatory synapse and spine density and weakened OD plasticity following MD (Kelly et al., 2015). Additionally, MMP9 regulates feed-forward thalamic inputs to the cortex (Murase et al., 2017). MMP2 and MMP9 proteolysis might mediate OD plasticity by promoting the weakening of excitatory synapses onto inhibitory neurons and strengthening of excitatory synapses onto excitatory neurons (Murase et al., 2017). Typically, the growth and strengthening of excitatory synapses onto excitatory neurons are linked to MMP9 (Kaliszewska et al., 2012; Ganguly et al., 2013; Lebida and Mozrzymas, 2017), but the weakening of thalamic inputs to fast-spiking interneurons was only recently associated with MMP9 (Murase et al., 2017). Although this report of MMP9 effect on disinhibition is very intriguing, it is important to note that there is a complex relationship between ECM integrity and neuronal excitability, which varies across brain regions, and depends on the PNN composition of the region (Murase et al., 2017). Nonetheless, MMP2 and MMP9 might be involved in the modulation of neuronal excitability in adult OD plasticity.

Adult SC-raised mice usually display OD plasticity after 7 d of MD until P110 (Gordon and Stryker, 1996; Lehmann and Löwel,

2008; Sato and Stryker, 2008). As previously reported, one of the mechanisms by which MMP9 might mediate adult OD plasticity is elevated proteolytic activity at thalamic inputs to the visual cortex on experience-dependent neuronal activity (Murase et al., 2017), where effects on various components of the ECM including gelatin, aggrecan, laminin, and collagen are exerted (Ethell and Ethell, 2007; Huntley, 2012). Thus, inhibition of proteolytic activity of gelatinases may lead to a severe impairment of plasticity. Moreover, structural and functional OD plasticity was absent in MMP9 knock-out mice, and rescued by hyaluronidase, that degrades key components of the ECM (Murase et al., 2017). To address the effect of MMP2/MMP9 inhibition on the degradation of ECM, we have utilized WFA staining of PNNs, which are specific ECM structures responsible for synaptic stabilization in the adult brain. Our data show that the daily administration of SB3CT led to significantly higher PNN counts in V1, i.e., reduced ECM degradation as shown by WFA staining, compared with vehicle-injected control mice. These results indicate that MMP2/9 play an important role in the organization of PNNs in the visual cortex, and the loss of their enzymatic activity might lead to a less permissive local environment, which subsequently affects OD plasticity. Our results further emphasize that MMP2/9 is indispensable for extracellular proteolysis in response to increased neuronal activity to reorganize a nonpermissive ECM into a plasticity-accommodating local environment (Milward et al., 2007; Gundelfinger et al., 2010; Huntley, 2012).

May other MMPs be also involved in visual plasticity? Notably, MMP3 is also expressed in the visual cortex, and cleaves and activates both MMP2 and MMP9 (Ogata et al., 1992; Gonthier et al., 2007). In the visual cortex of MMP3-deficient mice, neuronal morphology is aberrant (Aerts et al., 2015). However, the morphologic and functional consequences observed in MMP3-deficient mice might be largely because of reduced activation of MMP2 and MMP9 by MMP3. Aerts and colleagues remark on the reduced pro-MMP9 activation on MMP3 knock-out (Johnson et al., 2011) and suggest MMP9 as the actual effector for the observed shift in spine length distribution toward shorter, more mature spines. Consistently, MMP9 increases spine lengthening and is necessary to maintain LTP, and is upregulated on synaptic activity (Nagy et al., 2006; Ethell and Ethell, 2007). Moreover, inhibition of MMP2 and MMP9 in our own paradigm likely induces complex cellular cascades, including compensatory upregulation of other redundant MMPs that can activate ODP to a lesser extent, which is not possible when using a broad spectrum inhibitor (Pielecka-Fortuna et al., 2015). Consistent with this hypothesis, MMP9 deficiency was shown to lead to a compensatory increase in MMP8 expression (Chiao et al., 2012).

Additionally, brain-derived neurotrophic factor (BDNF) is one of the factors implicated in interactions with both MMP2/9 activity and synaptic plasticity (Lu and Martinowich, 2008; Kuzniewska et al., 2013). BDNF expression and MMP2/9 activity are upregulated on neuronal activity (Ethell and Ethell, 2007; Kuzniewska et al., 2013; Reinhard et al., 2015). Interestingly, proteolytic conversion of proBDNF (proform) to mBDNF (mature BDNF) is processed by MMP2 and MMP9, among others (Lee et al., 2001; Hwang et al., 2005; Ethell and Ethell, 2007). Notably, proBDNF and mBDNF elicit opposite biological effects by activating two distinct receptor systems: proBDNF promotes long-term depression (LTD) through the activation of p75 receptor in the hippocampus, while mBDNF-TrkB signaling is critical for the early phase of LTP (Lohof et al., 1993; Chao and Bothwell, 2002; Lu, 2003; Yang et al., 2009). BDNF is upstream of the

←

circles) did not show OD plasticity (D). In contrast, a single injection of the MMP2/9 inhibitor SB3CT after the PT lesion rescued OD plasticity so that MD induced a strong OD shift toward the nondeprived eye (ipsilateral; E). Likewise, in sham-lesioned mice, neither vehicle nor SB3CT injections compromised OD plasticity, nor MD induced an OD shift toward the nondeprived eye (H, I). Data display same as Figure 1. Scale bars: 1 mm. Tables comparing the two independent analyses are provided as the Extended Data Figure 5-1.

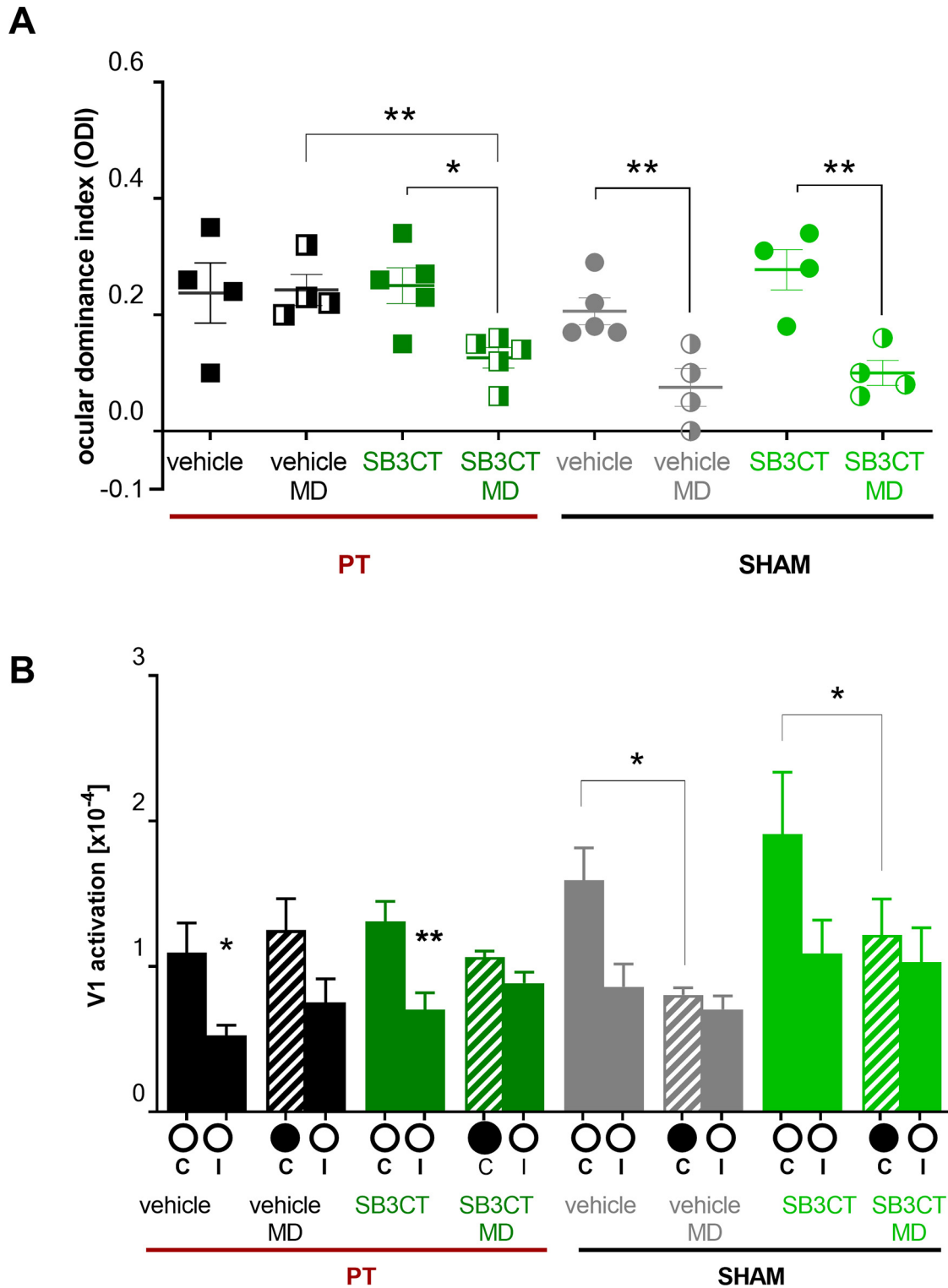


Figure 6. Quantification of OD plasticity on the brief (1-d) inhibition of MMP2/MMP9 with SB3CT after a PT lesion in S1: both ODIs (**A**) and V1 activation (**B**) without and with MD in the various treatment groups (vehicle/SB3CT and PT/sham lesion) are illustrated. **A**, Optically imaged ODIs of mice injected with vehicle (black/gray) or SB3CT (dark green, light green). Symbols represent ODI values of individuals (squares specify PT-lesioned mice, circles sham-lesioned mice). In PT mice with MD, a single systemic administration of SB3CT on d0 rescued the impaired OD shift (impaired by PT in vehicle-treated mice). **B**, V1 activation elicited by stimulation of the contralateral (C) or ipsilateral (I) eye without and after MD. Multivariate ANOVA, followed up by Sidak-corrected tests for simple effects. Data display as in Figure 2. Mean \pm SEM, * $p < 0.05$, ** $p < 0.01$, *** $p < 0.001$.

regulation of MMP9 expression and activity in neurons, yet MMP2 and MMP9 modulate BDNF activity in a feedforward cycle. Thus, accumulation of proBDNF because of the lack of MMP2/9 activity, caused by SB3CT, could negatively affect

neuronal remodeling and weaken activity dependent changes. Inhibition of MMP2 and MMP9, and consequent restriction of proteolytic activation of BDNF may therefore be contributing to the loss of V1 plasticity in adult SB3CT-treated mice. Future

Table 2. Optometry-measured contrast sensitivity comparisons of PT/sham groups before and after MD

Spatial frequency (cyc/°)	Contrast sensitivity		[100/(%value*0.985)]	
	PT_vehicle d0	PT_vehicle_MD	PT_SB3CT	PT_SB3CT_MD
0.031	3.7 ± 0.07	3.8 ± 0.07	3.8 ± 0.08	3.5 ± 0.03
0.064	12.2 ± 0.33	11.9 ± 0.15	11.6 ± 0.25	11.2 ± 0.66
0.092	11.5 ± 0.22	10.8 ± 8.93	10.7 ± 0.42	9.9 ± 0.56
0.103	10.3 ± 0.43	8.9 ± 0.10	9.8 ± 0.38	8.2 ± 0.41
0.192	7.4 ± 0.30	7.0 ± 0.17	7.6 ± 0.33	7.2 ± 0.31
0.272	3.8 ± 0.06	4.1 ± 0.05	4.0 ± 0.04	3.9 ± 0.08
	d7			
0.031	3.7 ± 0.07	3.8 ± 0.08	3.8 ± 0.09	4.4 ± 0.08
0.064	12.2 ± 0.33	12.0 ± 0.17	11.7 ± 0.17	23.5 ± 3.37
0.092	11.5 ± 0.22	11.1 ± 0.18	10.7 ± 0.42	21.2 ± 3.22
0.103	10.03 ± 0.43	9.0 ± 0.06	9.8 ± 0.38	16.1 ± 2.39
0.192	7.4 ± 0.30	7.1 ± 0.20	7.6 ± 0.33	14.5 ± 2.59
0.272	3.8 ± 0.06	4.2 ± 0.06	4.1 ± 0.04	5.0 ± 0.19
	Sham_vehicle d0		Sham_SB3CT	
0.031	3.7 ± 0.08	3.6 ± 0.08	3.8 ± 0.05	3.5 ± 0.03
0.064	11.9 ± 0.20	11.9 ± 0.19	11.9 ± 0.12	11.7 ± 0.16
0.092	10.7 ± 0.40	11.1 ± 0.23	11.2 ± 0.13	10.7 ± 0.37
0.103	9.7 ± 0.56	10.1 ± 0.31	9.8 ± 0.43	8.7 ± 0.36
0.192	7.3 ± 0.23	6.9 ± 0.15	6.9 ± 0.11	7.1 ± 0.35
0.272	3.9 ± 0.10	3.8 ± 0.01	3.9 ± 0.06	4.0 ± 0.01
	d7			
0.031	3.7 ± 0.08	4.6 ± 0.08	3.8 ± 0.05	4.1 ± 0.16
0.064	11.9 ± 0.20	22.3 ± 1.04	11.9 ± 0.09	18.7 ± 1.77
0.092	10.7 ± 0.40	21.7 ± 0.61	11.2 ± 0.13	17.7 ± 1.81
0.103	9.7 ± 0.56	19.8 ± 1.05	9.8 ± 0.43	13.2 ± 1.22
0.192	7.3 ± 0.23	11.2 ± 0.46	6.9 ± 0.11	10.3 ± 0.79
0.272	3.9 ± 0.10	5.1 ± 0.15	3.9 ± 0.06	4.8 ± 0.19

Table 3. Optometry-measured contrast sensitivity comparisons of running wheel (RW) groups before and after MD

Spatial frequency (cyc/deg)	Contrast sensitivity		[100/(%value*0.985)]
	Day 0		
	RW + Vehicle + MD	RW + SB3CT + MD	
0.031	3.75 ± 0.04	3.72 ± 0.04	
0.064	11.44 ± 0.06	11.99 ± 0.25	
0.092	10.98 ± 0.10	11.20 ± 0.17	
0.103	10.54 ± 0.26	10.69 ± 0.12	
0.192	7.38 ± 0.18	7.49 ± 0.15	
0.272	3.64 ± 0.03	3.63 ± 0.03	
	Day 7		
0.031	4.63 ± 0.07	4.16 ± 0.06	
0.064	21.28 ± 0.34	15.27 ± 0.98	
0.092	20.21 ± 0.25	14.11 ± 1.05	
0.103	19.17 ± 0.25	13.26 ± 0.89	
0.192	11.21 ± 0.26	9.09 ± 0.26	
0.272	4.47 ± 0.08	4.01 ± 0.08	

experiments should elucidate the mechanism of MMP2 and MMP9 action in relation to BDNF signaling for OD plasticity in adult and juvenile mice.

MMP2/9 in disease

As discussed, MMP2 and MMP9 activity support healthy brain development and function, while excess enzymatic activity can have deleterious consequences after brain injury or disease (Agrawal et al., 2008; Huntley, 2012). The expression of many MMPs has been reported to change in response to injury or neurologic diseases (Yong, 2005; Reinhard et al., 2015). In the barrel cortex, MMP activity increased within 24 h of a PT-induced

stroke, and treatment with a broad-spectrum MMP inhibitor during stroke induction partially recovered lesion-diminished plasticity (Cybulska-Klosowicz et al., 2011; Liguz-Lecznar et al., 2012). Similarly, our laboratory has previously shown that compromised plasticity in the visual cortex after a localized cortical stroke in S1 (Greifzu et al., 2011) was rescued by a 1-d treatment with a broad-spectrum MMP inhibitor after stroke induction (Pielecka-Fortuna et al., 2015). Although studies using broad-spectrum inhibitors yielded promising results in animal models of stroke, their low specificity and systemic toxicity makes their translational use difficult if not impossible (Coussens et al., 2002; López-Otín and Overall, 2002; Gu, 2005). More specific treatment options are therefore strongly needed. Notably, MMP9 shows increased expression after stroke in humans (Castellanos et al., 2003; Horstmann et al., 2003; Gu, 2005), nonhuman primates (Heo et al., 1999), and rodents (Romanic et al., 1998; Fujimura et al., 1999; Justicia et al., 2003), which has been linked to numerous complications including excitotoxicity, neuronal damage, apoptosis, blood brain barrier disruption, and neuroinflammation (Chaturvedi and Kaczmarek, 2014). Furthermore, prolonged MMP2-mediated proteolysis has been implicated in many CNS injuries (Justicia et al., 2003; Huntley, 2012). While upregulation of specific MMPs is highly dependent on the type, localization, and strength of the ischemic insult (Turner and Sharp, 2016), particularly the expression of MMP2 and MMP9 is altered following stroke and traumatic brain injury, causing alterations in blood-brain barrier permeability (Romanic et al., 1998; Fujimura et al., 1999; Planas et al., 2001). Importantly, a cortical stroke elevates activity of MMPs not only in the infarct tissue, but also in regions surrounding the infarct (Rosell et al., 2006; Dong et al., 2009). Here, the focal stroke induction was induced in the S1, in

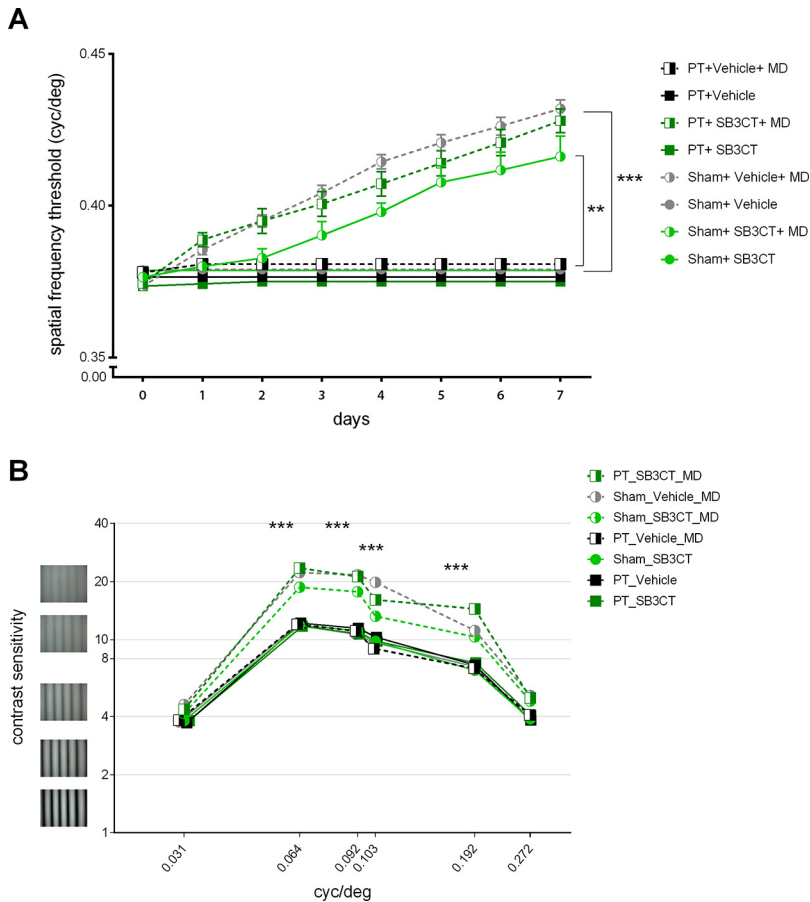


Figure 7. Injection of the MMP2/9 inhibitor SB3CT after the induction of a PT lesion in S1 rescued experience-enabled enhancements of both the spatial frequency (**A**) and contrast sensitivity (**B**) thresholds of the optomotor reflex in adult mice. **A**, Spatial frequency threshold values in cyc/deg are plotted against days for PT (squares), sham (circles), in mice without (filled symbols) and with MD (half-filled symbols), both for vehicle (black/gray) and SB3CT (dark green, light green) treatment. Seven days of MD induced a significant increase in spatial frequency threshold in SB3CT-injected PT-treated mice each day but not in vehicle-injected PT mice. In contrast, sham-lesioned mice showed significant threshold increases over days after MD (half-filled squares) compared with noMD mice, regardless of the type of injection (vehicle/SB3CT). **B**, Likewise, SB3CT treatment after PT rescued the experience-induced increase in contrast sensitivity thresholds of the open eye after MD: PT mice receiving a single SB3CT injection (dark green) had higher contrast thresholds, while the contrast thresholds of vehicle-treated PT mice (black) were significantly lower compared with SB3CT-injected PT mice. Sham-lesioned MD mice also had significantly higher contrast thresholds at every spatial frequency compared with noMD mice, regardless of treatment (vehicle and SB3CT). Gratings left of the y-axis illustrate the contrast steps for a given (constant) spatial frequency. Mixed ANOVA followed up by Sidak-corrected test for simple effects. Mean \pm SEM, * $p < 0.05$, ** $p < 0.01$, *** $p < 0.001$.

the close vicinity of V1, which is in the peri-infarct area. Notably, we show here that selective inhibition of MMP2 and MMP9 was sufficient to recover OD plasticity in the visual cortex after an S1 stroke in adult mice.

Interestingly, administration of SB3CT had failed to provide protection against a hypoxic ischemic insult in neonatal rats (Ranasinghe et al., 2012). This is in line with our observations of the unchanged lesion size in PT mice on the inhibition of MMP2/9. In our paradigm, we have induced a lesion in the S1, and tested the rescue of OD plasticity in the distant V1 on MMP2/9 inhibition. Unchanged lesion size and rescue of impaired OD plasticity indicate that neuroprotection after a stroke and recovery of plasticity near the lesion might be differentially mediated, and require different temporal regulation of MMP2 and MMP9 activity.

The comparison of our results with the literature highlights the complexity of finding an adequate treatment for recovery following an ischemic stroke that would both minimize the lesion

size and rescue the cortical plasticity. Regarding potential clinical relevance of SB3CT, our present results show that a single dose of SB3CT 24 h within stroke induction was able to rescue otherwise compromised plasticity are very encouraging; still, future experiments should test whether downregulation of excessive MMP2 and MMP9 activity even later after stroke could also act therapeutically.

Excessive and protracted MMP2 and MMP9 mediated proteolysis has been shown to be a major pathologic element of many CNS injuries and diseases (Huntley, 2012). There are several potential mechanisms by which elevated levels of MMPs may disrupt OD plasticity after a stroke in S1. It is for example plausible that MMP2 and MMP9 inhibition rescue OD plasticity after a stroke induction in S1 by impeding the negative effects of disrupted homeostasis early on. For instance, one of the consequences of MMP9 upregulation on brain damage is excessive degradation of the ECM protein laminin, which leads to neuronal apoptosis (Gu, 2005). Inhibiting overexpression of MMP2 and MMP9 after PT might contribute to the observed rescue of OD plasticity, possibly by protecting against laminin degradation and subsequent neuronal cell death. Additionally, induction of an ischemic insult leads to a propagating wave of neuronal and glial depolarization, called cortical spreading depression (Schroeter et al., 1995). Spreading depression alters blood brain barrier permeability by activating MMP9 (Gursoy-Ozdemir et al., 2004), and it might contribute to impairment of OD plasticity as well. It is possible that inhibition of MMP2/9 shortly after stroke induction could reduce spreading depression in the cortex, contributing to the rescued visual plasticity. Additionally, after a focal stroke, the balance of neuronal inhibition and excitation is disrupted, and neuron hyperexcitability on elevated levels of glutamate and reduction of GABAergic receptors are observed in peri-infarct regions, which is hypothesized to also lead to subsequent excitotoxicity and cell death (Neumann-Haefelin et al., 1995; Schiene et al., 1996; Murphy and Corbett, 2009). Thus, it is conceivable that treatment with the MMP2 and MMP9 inhibitor SB3CT shortly after the stroke downregulated these elevated MMPs, improved disrupted excitation/inhibition balance and contributed to the rescue of OD plasticity in the visual cortex, which can be interpreted as located in the peri-infarct region of the stroke in S1.

In our study, we have also investigated the behavioral relevance of MMP2 and MMP9 in visual capabilities of mice. Under normal conditions, daily testing in the optomotor setup after MD induces a cortex-dependent and experience-enabled enhancement of spatial vision through the nondeprived eye (Prusky et al., 2006). Here, we report that MMP2/9 inhibition during the MD period suppressed enhancements in both the spatial frequency and contrast

sensitivity thresholds of the optomotor reflex, while control mice displayed the typical experience-enabled improvements in spatial vision. Conversely, the brief inhibition of MMP2/MMP9 immediately after a cortical stroke rescued otherwise impaired optomotor improvements. Our results thus indicate that MMP2/9 have nonredundant functions in both OD plasticity and activity-dependent improvements of visual abilities in adult mice.

Together, the present data considerably extend our previous findings, emphasizing an important regulatory role of MMP2/9 for preserving adult cortical plasticity: reduction of MMP2/9 activity blocked plasticity in healthy adult mice, while suppressing overactivity that occurs after a cortical lesion rescued otherwise compromised plasticity. We would like to highlight that it is very encouraging for the development of clinically relevant therapeutic approaches that already a single treatment with the selective MMP2/9 inhibitor briefly after lesion induction rescued plasticity in the adult brain.

References

- Aerts J, Nys J, Moons L, Hu TT, Arckens L (2015) Altered neuronal architecture and plasticity in the visual cortex of adult MMP-3-deficient mice. *Brain Struct Funct* 220:2675–2689.
- Agrawal S, Lau L, Yong V (2008) MMPs in the central nervous system: where the good guys go bad. *Semin Cell Dev Biol* 19:42–51.
- Asahi M, Wang X, Mori T, Sumii T, Jung JC, Moskowitz MA, Fini ME, Lo EH (2001) Effects of matrix metalloproteinase-9 gene knock-out on the proteolysis of blood-brain barrier and white matter components after cerebral ischemia. *J Neurosci* 21:7724–7732.
- Berardi N, Pizzorusso T, Maffei L (2004) Extracellular matrix and visual cortical plasticity: freeing the synapse. *Neuron* 44:905–908.
- Bonfil RD, Sabbota A, Nabha S, Bernardo MM, Dong Z, Meng H, Yamamoto H, Chinni SR, Lim IT, Chang M, Filetti LC, Mobashery S, Cher ML, Fridman R (2006) Inhibition of human prostate cancer growth, osteolysis and angiogenesis in a bone metastasis model by a novel mechanism-based selective gelatinase inhibitor. *Int J Cancer* 118:2721–2726.
- Brown S, Bernardo MM, Li Z-H, Kotra LP, Tanaka Y, Fridman R, Mobashery S (2000) Potent and selective mechanism-based inhibition of gelatinases. *J Am Chem Soc* 122:6799–6800.
- Cai H, Ma Y, Jiang L, Mu Z, Jiang Z, Chen X, Wang Y, Yang GY, Zhang Z (2017) Hypoxia response element-regulated MMP-9 promotes neurological recovery via glial scar degradation and angiogenesis in delayed stroke. *Mol Ther* 25:1448–1459.
- Cang J, Renteria RC, Kaneko M, Liu X, Copenhagen DR, Stryker MP (2005) Development of precise maps in visual cortex requires patterned spontaneous activity in the retina. *Neuron* 48:797–809.
- Castellanos M, Leira R, Serena J, Pumar JM, Lizasoain I, Dávalos A (2003) Plasma metalloproteinase-9 concentration predicts hemorrhagic transformation in acute ischemic stroke. *Stroke* 34:40–46.
- Chao MV, Bothwell M (2002) Neurotrophins: to cleave or not to cleave. *Neuron* 33:9–12.
- Chaturvedi M, Kaczmarek L (2014) MMP-9 inhibition: a therapeutic strategy in ischemic stroke. *Mol Neurobiol* 49:563–573.
- Chiao YA, Ramirez TA, Zamilpa R, Okoronkwo SM, Dai Q, Zhang J, Jin Y-F, Lindsey ML (2012) Matrix metalloproteinase-9 deletion attenuates myocardial fibrosis and diastolic dysfunction in ageing mice. *Cardiovasc Res* 96:444–455.
- Coussens LM, Fingleton B, Matrisian LM (2002) Matrix metalloproteinase inhibitors and cancer: trials and tribulations. *Science* 295:2387–2392.
- Cui J, Chen S, Zhang C, Meng F, Wu W, Hu R, Hadass O, Lehmidi T, Blair GJ, Lee M, Chang M, Mobashery S, Sun GY, Gu Z (2012) Inhibition of MMP-9 by a selective gelatinase inhibitor protects neurovasculature from embolic focal cerebral ischemia. *Mol Neurodegener* 7:21.
- Cybulska-Klosowicz A, Liguz-Leczna M, Nowicka D, Ziemka-Nalczyk M, Kossut M, Skangiel-Kramska J (2011) Matrix metalloproteinase inhibition counteracts impairment of cortical experience-dependent plasticity after photothrombotic stroke. *Eur J Neurosci* 33:2238–2246.
- Dityatev A, Schachner M, Sonderegger P (2010) The dual role of the extracellular matrix in synaptic plasticity and homeostasis. *Nat Rev Neurosci* 11:735–746.
- Dong X, Song YN, Liu WG, Guo XL (2009) MMP-9, a potential target for cerebral ischemic treatment. *Curr Neuropharmacol* 7:269–275.
- Dräger UC (1978) Observations on monocular deprivation in mice. *J Neurophysiol* 41:28–42.
- Espinosa JS, Stryker MP (2012) Development and plasticity of the primary visual cortex. *Neuron* 75:230–249.
- Ethell IM, Ethell DW (2007) Matrix metalloproteinases in brain development and remodeling: synaptic functions and targets. *J Neurosci Res* 85:2813–2823.
- Frenkel MY, Bear MF (2004) How monocular deprivation shifts ocular dominance in visual cortex of young mice. *Neuron* 44:917–923.
- Frischknecht R, Gundelfinger ED (2012) The brain's extracellular matrix and its role in synaptic plasticity. *Adv Exp Med Biol* 970:153–171.
- Fujimura M, Gasche Y, Morita-Fujimura Y, Massengale J, Kawase M, Chan PH (1999) Early appearance of activated matrix metalloproteinase-9 and blood-brain barrier disruption in mice after focal cerebral ischemia and reperfusion. *Brain Res* 842:92–100.
- Ganguly K, Rejmak E, Mikosz M, Nikolaev E, Knapska E, Kaczmarek L (2013) Matrix metalloproteinase (MMP) 9 transcription in mouse brain induced by fear learning. *J Biol Chemistry* 288:20978–20991.
- Gonthier B, Nasarre C, Roth L, Perraut M, Thomasset N, Roussel G, Aunis D, Bagnard D (2007) Functional interaction between matrix metalloproteinase-3 and semaphorin-3C during cortical axonal growth and guidance. *Cereb Cortex* 17:1712–1721.
- Gordon JA, Stryker MP (1996) Experience-dependent plasticity of binocular responses in the primary visual cortex of the mouse. *J Neurosci* 16:3274–3286.
- Greifzu F, Schmidt S, Schmidt KF, Kreikemeier K, Witte OW, Löwel S (2011) Global impairment and therapeutic restoration of visual plasticity mechanisms after a localized cortical stroke. *Proc Natl Acad Sci USA* 108:15450–15455.
- Greifzu F, Pielecka-Fortuna J, Kalogeraki E, Krempler K, Favaro PD, Schlüter OM, Löwel S (2014) Environmental enrichment extends ocular dominance plasticity into adulthood and protects from stroke-induced impairments of plasticity. *Proc Natl Acad Sci USA* 111:1150–1155.
- Gu Z, Cui J, Brown S, Fridman R, Mobashery S, Strongin AY, Lipton SA (2005) A highly specific inhibitor of matrix metalloproteinase-9 rescues laminin from proteolysis and neurons from apoptosis in transient focal cerebral ischemia. *J Neurosci* 25:6401–6408.
- Gundelfinger ED, Frischknecht R, Choquet D, Heine M (2010) Converting juvenile into adult plasticity: a role for the brain's extracellular matrix. *Eur J Neurosci* 31:2156–2165.
- Gursoy-Ozdemir Y, Qiu J, Matsuoka N, Bolay H, Bermppohl D, Jin H, Wang X, Rosenberg GA, Lo EH, Moskowitz MA (2004) Cortical spreading depression activates and upregulates MMP-9. *J Clin Invest* 113:1447–1455.
- Härtig W, Brauer K, Brückner G (1992) Wisteria floribunda agglutinin-labelled nets surround parvalbumin-containing neurons. *Neuroreport* 3:869–872.
- Heo JH, Lucero J, Abumiyi T, Koziol JA, Copeland BR, del Zoppo GJ (1999) Matrix metalloproteinases increase very early during experimental focal cerebral ischemia. *J Cereb Blood Flow Metab* 19:624–633.
- Hofer SB, Mrcic-Flogel TD, Bonhoeffer T, Hübener M (2006) Lifelong learning: ocular dominance plasticity in mouse visual cortex. *Curr Opin Neurobiol* 16:451–459.
- Horstmann S, Kalb P, Koziol J, Gardner H, Wagner S (2003) Profiles of matrix metalloproteinases, their inhibitors, and laminin in stroke patients: influence of different therapies. *Stroke* 34:2165–2170.
- Hubel DH, Wiesel TN (1962) Receptive fields, binocular interaction and functional architecture in the cat's visual cortex. *J Physiol* 160:106–154.

- Huntley GW (2012) Synaptic circuit remodelling by matrix metalloproteinases in health and disease. *Nat Rev Neurosci* 13:743–757.
- Hwang JJ, Park M-H, Choi S-Y, Koh J-Y (2005) Activation of the Trk signaling pathway by extracellular zinc. Role of metalloproteinases. *J Biol Chem* 280:11995–12001.
- Jia F, Yin YH, Gao GY, Wang Y, Cen L, Jiang JY (2014) MMP-9 inhibitor SB-3CT attenuates behavioral impairments and hippocampal loss after traumatic brain injury in rat. *J Neurotrauma* 31:1225–1234.
- Johnson JL, Dwivedi A, Somerville M, George SJ, Newby AC (2011) Matrix metalloproteinase (MMP)-3 activates MMP-9 mediated vascular smooth muscle cell migration and neointima formation in mice. *Arterioscler Thromb Vasc Biol* 31:e35–e44.
- Justicia C, Panés J, Solé S, Cervera A, Deulofeu R, Chamorro A, Planas AM (2003) Neutrophil infiltration increases matrix metalloproteinase-9 in the ischemic brain after occlusion/reperfusion of the middle cerebral artery in rats. *J Cereb Blood Flow Metab* 23:1430–1440.
- Kaliszewska A, Bijata M, Kaczmarek L, Kossut M (2012) Experience-dependent plasticity of the barrel cortex in mice observed with 2-DG brain mapping and c-Fos: Effects of MMP-9 KO. *Cereb Cortex* 22:2160–2170.
- Kalatsky VA, Stryker MP (2003) New paradigm for optical imaging: temporally encoded maps of intrinsic signal. *Neuron* 38:529–545.
- Kalogeraki E, Pielecka-Fortuna J, Hüppe JM, Löwel S (2016) Physical exercise preserves adult visual plasticity in mice and restores it after a stroke in the somatosensory cortex. *Front Aging Neurosci* 8:212.
- Kelly EA, Russo AS, Jackson CD, Lamantia CE, Majewska AK (2015) Proteolytic regulation of synaptic plasticity in the mouse primary visual cortex: analysis of matrix metalloproteinase 9 deficient mice. *Front Cell Neurosci* 9:369.
- Kuzniewska B, Rejmak E, Malik AR, Jaworski J, Kaczmarek L, Kalita K (2013) Brain-derived neurotrophic factor induces matrix metalloproteinase 9 expression in neurons via the serum response factor/c-Fos pathway. *Mol Cell Biol* 33:2149–2162.
- Lai TW, Zhang S, Wang YT (2014) Excitotoxicity and stroke: identifying novel targets for neuroprotection. *Prog Neurobiol* 115:157–188.
- Lebeda K, Mozrzymas JW (2017) Spike timing-dependent plasticity in the mouse barrel cortex is strongly modulated by sensory learning and depends on activity of matrix metalloproteinase 9. *Molec Neurobiol* 54:6723–6736.
- Lee R, Kermani P, Teng KK, Hempstead BL (2001) Regulation of cell survival by secreted proneurotrophins. *Science* 294:1945–1948.
- Lehmann K, Löwel S (2008) Age-dependent ocular dominance plasticity in adult mice. *PLoS One* 3:e3120.
- Levitt CN, Hübener M (2012) Critical-period plasticity in the visual cortex. *Annu Rev Neurosci* 35:309–330.
- Liguz-Leczna M, Ziemka-Nalecz M, Aleksy M, Kossut M, Skangiel-Kramska J, Nowicka D (2012) Comparison of matrix metalloproteinase activation after focal cortical ischemia in young adult and aged mice. *J Neurosci Res* 90:203–212.
- Lohof AM, Ip NY, Poo MM (1993) Potentiation of developing neuromuscular synapses by the neurotrophins NT-3 and BDNF. *Nature* 363:350–353.
- López-Otín C, Overall CM (2002) Protease degradomics: a new challenge for proteomics. *Nat Rev Mol Cell Biol* 3:509–519.
- Lu B (2003) BDNF and activity-dependent synaptic modulation. *Learn Mem* 10:86–98.
- Lu B, Martinowich K (2008) Cell biology of BDNF and its relevance to schizophrenia. *Novartis Found Symp* 289:119–129; discussion 129–135, 193–195.
- Meighan SE, Meighan PC, Choudhury P, Davis CJ, Olson ML, Zornes PA, Wright JW, Harding JW (2006) Effects of extracellular matrix-degrading proteases matrix metalloproteinases 3 and 9 on spatial learning and synaptic plasticity. *J Neurochem* 96:1227–1241.
- Milward EA, Fitzsimmons C, Szklarczyk A, Conant K (2007) The matrix metalloproteinases and CNS plasticity: an overview. *J Neuroimmunol* 187:9–19.
- Murase S, Lantz CL, Quinlan EM (2017) Light reintroduction after dark exposure reactivates plasticity in adults via perisynaptic activation of MMP-9. *Elife* 6:e27345.
- Murphy TH, Corbett D (2009) Plasticity during stroke recovery: from synapse to behaviour. *Nat Rev Neurosci* 10:861–872.
- Nagy V, Bozdagi O, Matyña A, Balcerzyk M, Okulski P, Dzwonek J, Costa RM, Silva AJ, Kaczmarek L, Huntley GW (2006) Matrix metalloproteinase-9 is required for hippocampal late-phase long-term potentiation and memory. *J Neurosci* 26:1923–1934.
- Neumann-Haefelin T, Hagemann G, Witte OW (1995) Cellular correlates of neuronal hyperexcitability in the vicinity of photochemically induced cortical infarcts in rats in vitro. *Neurosci Lett* 193:101–104.
- Ogata Y, Enghild JJ, Nagase H (1992) Matrix metalloproteinase 3 (stromelysin) activates the precursor for the human matrix metalloproteinase 9. *J Biol Chem* 267:3581–3584.
- Paxinos G, Franklin KBJ (2001) *The Mouse Brain in Stereotaxic Coordinates*. Ed 2. San Diego:Academic Press.
- Pielecka-Fortuna J, Kalogeraki E, Fortuna MG, Löwel S (2015) Optimal level activity of matrix metalloproteinases is critical for adult visual plasticity in the healthy and stroke-affected brain. *Elife* 5:e11290.
- Pizzorusso T, Medini P, Berardi N, Chierzi S, Fawcett JW, Maffei L (2002) Reactivation of ocular dominance plasticity in the adult visual cortex. *Science* 298:1248–1251.
- Pizzorusso T, Medini P, Landi S, Baldini S, Berardi N, Maffei L (2006) Structural and functional recovery from early monocular deprivation in adult rats. *Proc Natl Acad Sci USA* 103:8517–8522.
- Planas AM, Solé S, Justicia C (2001) Expression and activation of matrix metalloproteinase-2 and -9 in rat brain after transient focal cerebral ischemia. *Neurobiol Dis* 8:834–846.
- Prusky GT, Alam NM, Beekman S, Douglas RM (2004) Rapid quantification of adult and developing mouse spatial vision using a virtual optomotor system. *Invest Ophthalmol Vis Sci* 45:4611–4616.
- Prusky GT, Alam NM, Douglas RM (2006) Enhancement of vision by monocular deprivation in adult mice. *J Neurosci* 26:11554–11561.
- Ranasinghe HS, Scheepens A, Sirimanne E, Mitchell MD, Williams CE, Fraser M (2012) Inhibition of MMP-9 activity following hypoxic ischemia in the developing brain using a highly specific inhibitor. *Dev Neurosci* 34:417–427.
- Reinhard SM, Razak K, Ethell IM (2015) A delicate balance: role of MMP-9 in brain development and pathophysiology of neurodevelopmental disorders. *Front Cell Neurosci* 9:280.
- Romanic AM, White RF, Arleth AJ, Ohlstein EH, Barone FC (1998) Matrix metalloproteinase expression increases after cerebral focal ischemia in rats: inhibition of matrix metalloproteinase-9 reduces infarct size. *Stroke* 29:1020–1030.
- Rosell A, Ortega-Aznar A, Alvarez-Sabín J, Fernández-Cadenas I, Ribó M, Molina CA, Lo EH, Montaner J (2006) Increased brain expression of matrix metalloproteinase-9 after ischemic and hemorrhagic human stroke. *Stroke* 37:1399–1406.
- Rosenberg GA (2002) Matrix metalloproteinases in neuroinflammation. *Glia* 39:279–291.
- Rosenberg GA, Estrada EY, Dencoff JE (1998) Matrix metalloproteinases and TIMPs are associated with blood-brain barrier opening after reperfusion in rat brain. *Stroke* 29:2189–2195.
- Sato M, Stryker MP (2008) Distinctive features of adult ocular dominance plasticity. *J Neurosci* 28:10278–10286.
- Sawtell NB, Frenkel MY, Philpot BD, Nakazawa K, Tonegawa S, Bear MF (2003) NMDA receptor-dependent ocular dominance plasticity in adult visual cortex. *Neuron* 38:977–985.
- Schiene K, Bruehl C, Zilles K, Qü M, Hagemann G, Kraemer M, Witte OW (1996) Neuronal hyperexcitability and reduction of GABAA-receptor expression in the surround of cerebral photothrombosis. *J Cereb Blood Flow Metab* 16:906–914.
- Schindelin J, Arganda-Carreras I, Frise E, Kaynig V, Longair M, Pietzsch T, Preibisch S, Rueden C, Saalfeld S, Schmid B, Tinevez J-Y, White DJ, Hartenstein V, Eliceiri K, Tomancak P, Cardona A (2012) Fiji: An open-source platform for biological-image analysis. *Nature Meth* 9:676–682.
- Schroeter M, Schiene K, Kraemer M, Hagemann G, Weigel H, Eysel UT, Witte OW, Stoll G (1995) Astroglial responses in photochemically induced focal ischemia of the rat cortex. *Exp Brain Res* 106:1–6.

- Spolidoro M, Putignano E, Munafò C, Maffei L, Pizzorusso T (2012) Inhibition of matrix metalloproteinases prevents the potentiation of non-deprived-eye responses after monocular deprivation in juvenile rats. *Cereb Cortex* 22:725–734.
- Turner RJ, Sharp FR (2016) Implications of MMP9 for blood brain barrier disruption and hemorrhagic transformation following ischemic stroke. *Front Cell Neurosci* 10:56.
- Watson BD, Dietrich WD, Busto R, Wachtel MS, Ginsberg MD (1985) Induction of reproducible brain infarction by photochemically initiated thrombosis. *Ann Neurol* 17:497–504.
- Wilczynski GM, Konopacki FA, Wilczek E, Lasiecka Z, Gorlewicz A, Michaluk P, Wawrzyniak M, Malinowska M, Okulski P, Kolodziej LR, Konopka W, Duniec K, Mioduszevska B, Nikolaev E, Walczak A, Owczarek D, Gorecki DC, Zuschratter W, Ottersen OP, Kaczmarek L (2008) Important role of matrix metalloproteinase 9 in epileptogenesis. *J Cell Biol* 180:1021–1035.
- Yang Y, Rosenberg GA (2015) Matrix metalloproteinases as therapeutic targets for stroke. *Brain Res* 1623:30–38.
- Yang J, Siao CJ, Nagappan G, Marinic T, Jing D, McGrath K, Chen ZY, Mark W, Tessarollo L, Lee FS, Lu B, Hempstead BL (2009) Neuronal release of proBDNF. *Nat Neurosci* 12:113–115.
- Yang Y, Candelario-Jalil E, Thompson JF, Cuadrado E, Estrada EY, Rosell A, Montaner J, Rosenberg GA (2010) Increased intranuclear matrix metalloproteinase activity in neurons interferes with oxidative DNA repair in focal cerebral ischemia. *J Neurochem* 112:134–149.
- Yong VW (2005) Metalloproteinases: mediators of pathology and regeneration in the CNS. *Nat Rev Neurosci* 6:931–944.